

Ira: Efficient Transaction Replay for Distributed Systems

Adithya Bhat
Visa Research
haxolotl.research@gmail.com

Harshal Shah
Visa Research
harshal.shah031@gmail.com

Mohsen Minaei
Visa Research
m.mohsen.minaei@gmail.com

Abstract

In primary-backup replication, consensus latency is bounded by the time for backup nodes to replay (re-execute) transactions proposed by the primary. In this work, we present Ira, a framework to accelerate backup replay by transmitting compact *hints* alongside transaction batches. Our key insight is that the primary, having already executed transactions, possesses knowledge of future access patterns which is exactly the information needed for optimal replay.

We use Ethereum for our case study and present a concrete protocol, Ira-L, within our framework to improve cache management of Ethereum block execution. The primaries implementing Ira-L provide hints that consist of the working set of keys used in an Ethereum block and one byte of metadata per key indicating the table to read from, and backups use these hints for efficient block replay.

We evaluated Ira-L against the state-of-the-art Ethereum client reth over two weeks of Ethereum mainnet activity (100,800 blocks containing over 24 million transactions). Our hints are compact, adding a median of 47 KB compressed per block ($\sim 5\%$ of block payload). We observe that the sequential hint generation and block execution imposes a 28.6% wall-time overhead on the primary, though the direct cost from hints is 10.9% of execution time; all of which can be pipelined and parallelized in production deployments. On the backup side, we observe that Ira-L achieves a median per-block speedup of $25\times$ over baseline reth. With 16 prefetch threads, aggregate replay time drops from 6.5 hours to 16 minutes ($23.6\times$ wall-time speedup).

1 Introduction

The primary-backup paradigm forms the cornerstone of fault-tolerant distributed systems, from traditional databases [35, 39] to modern blockchain networks [63, 69]. In the standard State Machine Replication (SMR) model [54], a designated *primary* executes batches of transactions and propagates them to *backup* replicas, who must replay these transactions to maintain consistent state.

We can decompose each transaction into a sequence of read and write operations against a key-value store. The primary executes these operations, leveraging caches and indexes to optimize performance. When propagating the transaction batch to backups, the current systems transmit only the transaction data itself, forcing each backup to independently reconstruct the execution path. Transmitting all read/write values would incur prohibitive bandwidth, whereas replaying compact transaction logs allows backups to independently reconstruct the state.

SMR protocols [42, 51] run a consensus protocol to ensure consistency of the state machine, but the latency of consensus depends on the response from a quorum of replicas (typically a majority or a super-majority). This makes replay critical to consensus performance.

This replay is inherently inefficient as the backups must make decisions (e.g., cache management) without knowledge of future access patterns, leading to sub-optimal eviction choices such as unnecessary waiting for I/O, redundant disk I/O, etc.

To illustrate this, consider a cache of size 2 containing keys $\{A, B\}$, with upcoming accesses C, A, C . When C arrives, we must evict one key. LRU evicts the least recently used key (A), causing a miss when we access A next. An optimal strategy would be to evict B avoiding the subsequent miss on A . Figure 1 illustrates this difference: LRU incurs 2 misses while optimal incurs only 1. Generalizing this, without knowledge of future accesses, backups using LRU or other heuristic policies cannot make these optimal decisions.

1.1 Our Approach: Hint-Based Replay

In the case where the exact access pattern is known, the optimal solution is the Belady [20, 45] algorithm for caching, which informally states that the optimal caching algorithm is to evict the keys that are used furthest from the current operation. Implementing it is traditionally impossible as the access pattern can never be determined *a priori*.

Our key insight is that the inefficiency from Fig. 1 stems

Operation	LRU Cache	Optimal Cache
Initial	{A,B}	{A,B}
access C	{B,C}	{A,C} <i>evict B</i>
access A	{C,A}	{A,C}
access C	{C,A}	{A,C}
Cache Misses	2	1
	 hit  miss	

Figure 1: LRU vs. Belady-optimal caching (cache size is 2). For access sequence C, A, C starting with cache $\{A, B\}$: LRU evicts A (least recently used) when C arrives, then misses when it accesses A next. Optimal evicts B (never accessed again), achieving one fewer miss. With hints, backups can make optimal eviction decisions.

from *information asymmetry*: the primary possesses complete knowledge of the access pattern but discards this information when communicating with backups. The primary can encode this knowledge compactly and transmit it as *hints* that enable backups to implement near-optimal replay. We propose Ira, a framework to accelerate replay through hint-based replay. Ira operates two components:

- **Primary.** This component executes transactions while recording keys and their accesses, producing a hint. The concrete details of the hints depend on the execution and storage details of the application. This component is also responsible for delivering the hint to the backups.
- **Backups.** This component replays transactions using the hint to improve the storage access. This component is also responsible for receiving the hints from the primary.

1.2 Contributions

In summary, we make the following contributions:

1. **Ethereum Case Study:** We systematically perform measurement studies on execution in Ethereum. We identify that I/O is a bottleneck, and caching plays a major role in improving the replay performance.
2. **Hint-Based Replay Architecture:** We design a system where the primary generates compact hints during execution that enable backups to implement optimal caching. Hints are advisory, i.e., incorrect hints affect performance but do not affect correctness, thus enabling incremental deployment.
3. **Ira for Ethereum.** We present Ira-L, which achieves optimal cache performance through per-block hints that enable Belady-optimal eviction.

4. **Performance evaluation:** We implement Ira by modifying the state-of-the-art Rust Ethereum implementation (reth) and demonstrate $24.9\times$ faster replay with only 10.9% hint generation overhead. With even a single backup node, Ira achieves net speedup; benefits grow with additional replicas.

Paper Organization. Section 2 presents our system model and the two-pass protocol. Section 4 describes the Ira-L algorithm. Section 5 presents experimental results. Section 6 discusses limitations and future work. Section 7 surveys related work, and Section 8 concludes.

2 Model and Preliminaries

Belady’s MIN Algorithm. Belady’s MIN algorithm [20], proved optimal by Mattson et al. [45], provides the theoretically optimal cache replacement policy: when eviction is necessary, evict the item whose next access is *furthest in the future*. This policy minimizes total cache misses but requires knowledge of future accesses; information that is typically unavailable. In primary-backup replication, however, the primary has already executed the workload and possesses this knowledge. Ira exploits this observation: the primary encodes future access information as *hints* that enable backups to implement near-optimal cache replacement.

2.1 Primary-backup system model

We assume the standard primary-backup replication model.

Primary Node. The primary executes transactions against a key-value store (e.g., MDBX) and proposes a batch of transactions for replication.

Backup Nodes. Backups receive transaction batches and associated metadata from the primary. The backups replay the transactions with standard configured cache policies (e.g., LRU). Backups independently verify execution results, ensuring correctness of primary’s proposal.

Execution Flow. A transaction batch proceeds through the system as follows:

1. The primary executes the batch, generating state updates.
2. The primary commits the batch to durable storage and transmits the log to backups.
3. Each backup replays the batch.
4. Backups acknowledge replay completion to the primary.

2.2 Ethereum: A Primer

Ethereum [63] is a decentralized blockchain platform that executes arbitrary programs called *smart contracts*. We provide background on the aspects relevant to understanding Ira-L; Section A describes the execution client architecture in detail.

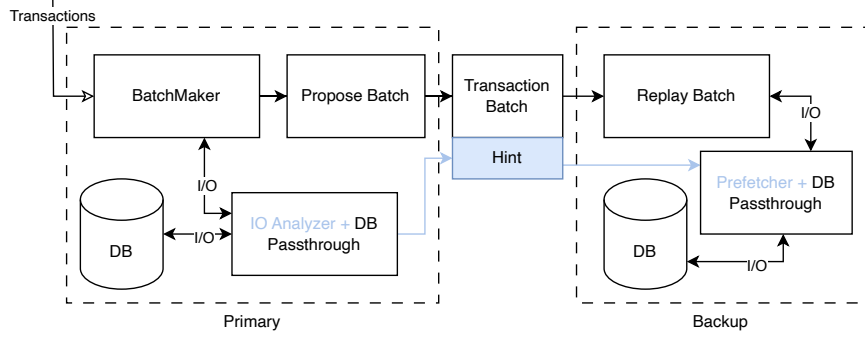


Figure 2: Ira architecture. The primary executes transactions while building a *hint* that records access information. Backups use these hints to implement optimal cache eviction during replay.

Client Architecture. Ethereum nodes run two cooperating clients: a *consensus client* that participates in the proof-of-stake protocol to determine the canonical chain, and an *execution client* that executes transactions and maintains state. The consensus client receives blocks from the network and instructs the execution client to validate them by re-executing all transactions and verifying the resulting state root.

Blocks and Transactions. A block contains an ordered sequence of transactions. Each transaction specifies a sender, recipient, value transfer, and optional calldata for smart contract invocation. The execution client processes transactions sequentially: each transaction observes the state modifications of all preceding transactions in the same block. This deterministic execution model ensures that all nodes converge to identical state.

State Model. Ethereum state is a mapping from 20-byte *addresses* to *accounts*. Each account contains:

- **Balance:** The account’s Ether holdings (256-bit integer)
- **Nonce:** A counter incremented with each outgoing transaction
- **Code:** For contract accounts, the immutable bytecode (up to 24 KB)
- **Storage:** For contract accounts, a mapping from 32-byte slots to 32-byte values

Contract storage is the dominant source of state I/O: a single contract may have millions of storage slots, and complex DeFi protocols access hundreds of slots per transaction.

Ethereum Virtual Machine (EVM). The EVM is a stack-based virtual machine that executes contract bytecode. State-accessing opcodes include:

- **SLOAD/SSTORE:** Read/write contract storage slots
- **BALANCE/SELFBALANCE:** Query account balances

- **CALL/STATICCALL/DELEGATECALL:** Invoke other contracts (loads bytecode)

- **EXTCODESIZE/EXTCODECOPY:** Query contract bytecode

Each state-accessing opcode translates to one or more database lookups in the execution client. Section 3 characterizes the distribution and locality of these operations.

Block Validation as Primary-Backup Replay. In Ethereum’s proof-of-stake consensus, a designated *proposer* (analogous to the primary) constructs and executes a new block, then broadcasts it to *validators* (analogous to backups). Validators must re-execute the block to verify correctness before attesting to it. This replay is the bottleneck that Ira-L addresses: the proposer has already executed the block and knows exactly which state will be accessed, but discards this information. Validators must independently discover the access pattern, incurring cache misses that the proposer could have predicted.

2.3 Ira: Hint-Based Replay Architecture

In the standard primary-backup model, the primary executes transactions and observes the complete access pattern, for instance which keys are read and written, in what order, but discards this information when propagating transactions to backups. Backups must independently reconstruct the access pattern during replay, making cache eviction decisions without knowledge of future accesses. This *information asymmetry* leads to suboptimal performance: backups incur cache misses that the primary could have predicted and prevented.

We bridge this asymmetry by having the primary encode its access pattern as a compact *hint* and transmit it alongside the transaction batch. The hint contains sufficient information for backups to prefetch required state before replay, eliminating cache misses. Critically, hints are *advisory*: they affect only performance, not correctness. If a hint is missing, corrupted, or incomplete, the backup falls back to standard replay without prefetching.

Protocol Overview. The Ira protocol operates in five phases:

1. **Primary Execution:** The primary executes transactions while instrumenting key accesses, recording each key read or written into an *access set* A .
2. **Hint Construction:** After execution, the primary constructs a hint H containing the access set A , optionally annotated with metadata (e.g., where to read each key, access ordering for Belady-optimal eviction).
3. **Hint Transmission:** The primary transmits H alongside (or ahead of) the transaction batch to backups.
4. **Backup Prefetch:** Backups use H to prefetch all keys in A into their cache before execution begins.
5. **Backup Replay:** Backups execute transactions with all required state pre-cached, achieving near-zero I/O latency during execution.

Hint Contents. At minimum, a hint contains the *access set* A : the set of unique keys accessed during batch execution. Richer hints may include additional metadata:

- **Source annotations:** Where to read each key (e.g., main state table vs. historical change sets), enabling the backup to route reads to the fastest storage path.
- **Access ordering:** The sequence in which keys are accessed, enabling Belady-optimal cache management when the access set exceeds cache capacity.
- **Read values:** The actual values read by the primary, trading bandwidth for backup computation when network capacity exceeds storage throughput.

The choice of hint granularity depends on the system’s I/O characteristics, network bandwidth, and memory constraints. Section 4 presents Ira-L, a concrete instantiation that uses per-block access sets with source annotations for Ethereum block replay. Section D discusses how to adapt Ira to other primary-backup systems including Raft-based databases, streaming replication, and distributed key-value stores.

Fault Tolerance. This architecture is agnostic to the underlying consensus or replication protocol. We rely on the underlying protocol, whether Paxos [42], Raft [51], or Byzantine fault-tolerant protocols like PBFT [?], for correctness guarantees. Ira is purely an optimization layer: hints do not affect the semantics of transaction execution or the safety properties of the replication protocol. A backup that receives incorrect or malicious hints may experience degraded performance (additional cache misses) but will never compute incorrect state.

3 Ethereum: A case study

Before designing Ira-L, we conduct a systematic characterization of Ethereum state access patterns to understand the structure and locality of block execution workloads.

3.1 Methodology

To characterize Ethereum state access patterns, we re-executed two weeks of historical mainnet blocks and recorded every state operation performed by the EVM. Re-execution against archival state ensures deterministic, reproducible traces that capture the exact sequence of operations from original block validation.

Instrumentation. We instrumented *reth* [12], a production Rust Ethereum client, using its EVM Inspector interface. The Inspector intercepts every EVM instruction during execution, allowing us to capture state operations at the exact moment they occur. For each state-accessing opcode, we perform *stack introspection* to extract operand values (target addresses, storage slots) directly from the EVM stack before the operation executes.

We capture 14 distinct operation types: storage operations (SLOAD, SSTORE), account metadata queries (BALANCE, SELFBALANCE, EXTCODESIZE, EXTCODEHASH), bytecode access (CALL, CALLCODE, STATICCALL, DELEGATECALL, EXTCODECOPY), and state modifications (CREATE, CREATE2, SELFDESTRUCT). Table 1 shows the trace database schema.

Table 1: Trace database schema for EVM state operations.

Field	Type	Description
block_number	uint64	Block containing operation
tx_index	uint16	Transaction position in block
op_index	uint32	Operation position in transaction
op_type	uint8	Operation type (14 types)
target_address	bytes20	Contract or account accessed
storage_slot	bytes32	Storage slot (nullable)
value_size	uint32	Bytecode size (nullable)

Block Processing. For each block, we retrieve the parent block’s state from reth’s archival database and execute all transactions sequentially. To ensure correct intra-block state visibility, we maintain a *write-through cache* that accumulates state modifications across transactions within a block: each transaction observes the effects of all preceding transactions, matching original execution semantics. Blocks are processed in parallel across CPU cores, with results merged and sorted by *(block, tx, op)* order.

Dataset. We collected traces from blocks 24,019,447 through 24,120,246 (100,800 consecutive blocks spanning two weeks of Ethereum mainnet activity). The trace contains 1,192,888,639 state operations across approximately 15 million transactions. We store traces in Apache Parquet [29] columnar format with Zstandard [26] compression, yielding a \sim 12 GB dataset.

Completeness. Our instrumentation captures 100% of state operations executed during block validation, with no sampling or filtering. Transactions that fail during re-execution (e.g., due to state inconsistencies) are excluded; these represent less than 0.01% of transactions and do not affect our findings.

Implementation Note. Reth uses flat storage (the PlainStorageState table in MDBX, a high-performance key-value store) for execution-time state access, rather than direct Merkle Patricia Trie traversal as specified by the Ethereum Yellow Paper [63]. Each SLOAD or SSTORE corresponds to a single key-value lookup. Our traces capture these logical operations, which directly correspond to database I/O during block execution.

3.2 Findings

#1. I/O dominates execution. State I/O overwhelmingly dominates block execution time rather than EVM computation. Figure 3 shows the breakdown of execution time across 100,800 consecutive blocks: I/O accounts for 67.9% of total execution time, while pure EVM computation consumes only 32.1%. The median per-block I/O share is 66.8%, with the 5-95th percentile range spanning 55.6%–80.2%, indicating consistent I/O dominance across blocks regardless of transaction volume.

This 2.1:1 of I/O-to-compute ratio has a critical implication: optimizing state access patterns yields far greater performance gains than optimizing EVM execution. Even a modest reduction in I/O latency—through caching, prefetching, or sequential access patterns—can substantially accelerate block validation.

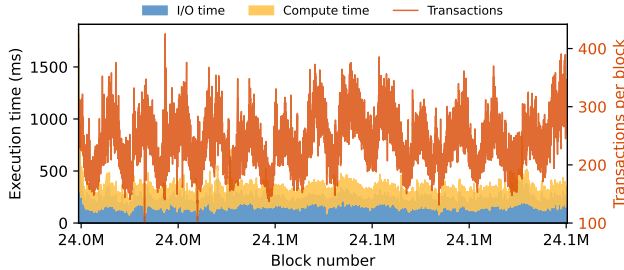


Figure 3: Execution time breakdown showing I/O dominance. The stacked area shows I/O time (blue) and compute time (yellow) per block; the line shows transaction count. I/O consistently dominates regardless of block size.

#2. Storage dominates I/O. Table 2 and Figure 4 show the distribution of state operations within the I/O operations in our trace. Storage operations (SLOAD and SSTORE) account for 75.6% of all state accesses. Call operations, while numerous, result in negligible bytecode I/O (~ 1 KB/block) because bytecode is immutable and cached effectively by the client. Account metadata queries comprise less than 1% of operations.

The read-write ratio for storage operations is 3.4 : 1 (696,683,837 SLOADs vs. 205,091,770 SSTOREs), indicating that reads dominate the workload. Since reads benefit directly

Table 2: State operation distribution across 100,800 blocks.

Category	Operations	Share
Storage (SLOAD/SSTORE)	901,775,607	75.6%
Calls (bytecode load)	281,933,575	23.6%
Account metadata	6,751,623	0.6%
Creation/destruction	2,427,834	0.2%
Total	1,192,888,639	100%

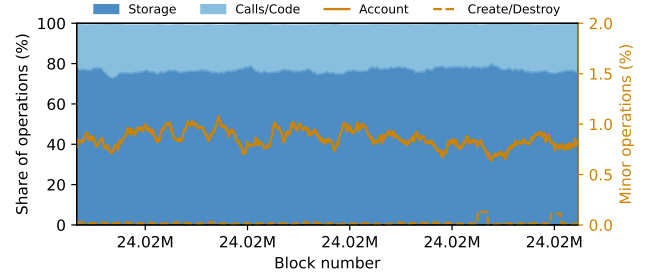


Figure 4: Per-block operation distribution showing storage dominance. Storage operations (blue) consistently account for the majority of state accesses across all blocks.

from cache hits while writes must persist regardless, this ratio suggests significant caching potential.

#3. High intra-block locality. We define the *reuse factor* as the ratio of total storage operations to unique storage keys accessed. Globally, the reuse factor is $25.74 \times (901,775,607)$ operations across 35,035,731 unique keys). However, this conflates intra-block and cross-block reuse.

To isolate intra-block locality, we examine the distribution of per-key access counts within blocks. Figure 5 shows this distribution: 34.5% of keys are accessed only once within their block, while 65.5% are accessed multiple times. The distribution exhibits a long tail, with some keys accessed up to 23,406 times within a single block.

This finding has important implications: we observe that 77.7% of key accesses within a block are to keys already accessed earlier in that block (i.e., of 901,876,518 storage accesses, only 200,839,090 are first accesses). A cache warmed with the correct keys before execution begins can serve most accesses as hits, thus underscoring the importance of an efficient caching system to improve block execution.

#4. Extreme Access Concentration. Access patterns exhibit extreme concentration at both the contract and key levels. Figure 6 shows the cumulative storage access share as a function of contract rank: the top 3 contracts (USDT, USDC, and Compound) account for 42.2% of all storage operations, and the top 10 contracts account for 63.6%. Table 6 in the appendix provides the detailed breakdown.

At the key level, concentration is even more pronounced.

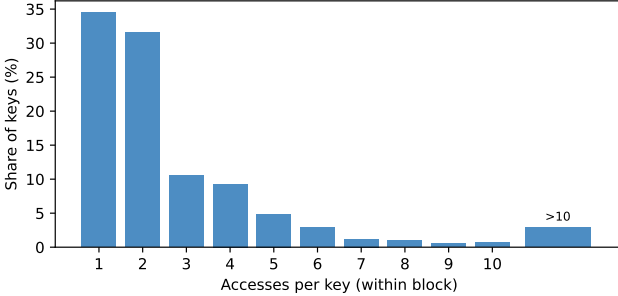


Figure 5: Intra-block access frequency distribution. Most keys are accessed 1–2 times per block, but a long tail of frequently-accessed keys drives high locality.

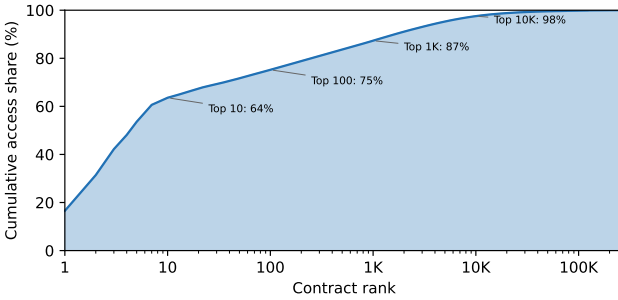


Figure 6: Cumulative storage access concentration by contract rank (out of 273,223 total contracts). A small number of contracts dominate state access: the top 10 contracts account for 63.6% and the top 10,000 account for 97.5% of all storage operations.

The top 1.23% of keys (430,873 keys with 100+ accesses) account for 84.0% of all storage operations. Conversely, 64% of keys are accessed only once or twice, contributing just 3.6% of total accesses.

#5. Ephemeral Key Dominance. Despite high intra-block reuse, most keys are ephemeral and appear in only one block. Figure 7 shows the distribution of key lifespans: 72.4% of keys appear in only a single block, and 21.4% appear in 2–5 blocks. Only 1.0% of keys persist across more than 50 blocks. Table 7 in the appendix provides the detailed breakdown.

Consecutive block overlap, i.e., the fraction of keys in block $n+1$ that also appeared in block n , averages only 12.4%, has a median of 11.7%, and a max of 100.0%. This low overlap implies that standard cache replacement policies like LRU cannot effectively predict which keys will be needed in upcoming blocks.

#6. Bounded Working Set. Figure 8 summarizes per-block statistics. The median block performs 8,629 total operations, of which 6,587 are storage operations accessing 1,806 unique

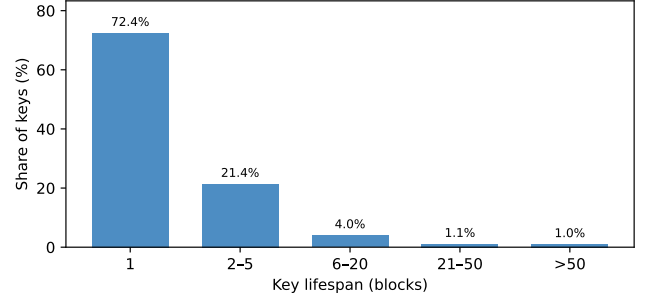


Figure 7: Key lifespan distribution: most keys are ephemeral and appear in only one block (72.4%), while less than 1.0% persist across more than 50 blocks.

keys. Even at the 95th percentile, blocks access only 3,920 unique keys. Table 8 in the appendix provides the detailed breakdown.

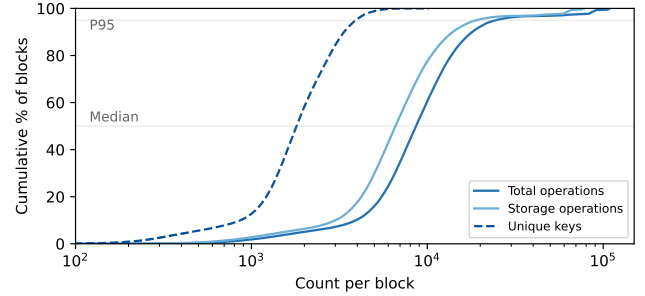


Figure 8: Cumulative distribution of per-block statistics. The working set remains bounded: 50% of blocks access fewer than 1,806 unique keys, and 95% access fewer than 3,920.

This bounded working set implies that per-block hints are tractable: hinting up to 2,000 keys requires at most 101 KB uncompressed (52 bytes per key: 20-byte address + 32-byte slot), which can be compressed significantly. The majority of blocks (58%) access fewer than 2,000 unique keys, and 84% access fewer than 3,000. Only 1.2% of blocks exceed 5,000 unique keys. This tight distribution suggests that a fixed-size hint buffer of 2,000–3,000 keys would cover the vast majority of blocks, making per-block prefetching hints both practical and efficient.

4 Ira-L: Latency-Optimal Algorithm

The workload analysis in Section 3 reveals four properties that jointly motivate Ira-L’s design. I/O accounts for 67.9% of block execution time (Finding #1), and storage operations dominate that I/O at 75.6% of all state accesses (Finding #2). The per-block working set is bounded, with a median of 1,806

unique keys (Finding #6), making per-block hints tractable. Yet 72.4% of keys are ephemeral, appearing in only a single block (Finding #5), and consecutive-block overlap averages just 12.4%. Hence, LRU and other heuristic replacement policies cannot effectively predict which keys the next block will need. The primary, however, already knows the complete access set for each block it executes. Discarding this information creates an unnecessary information asymmetry between primary and backup.

Ira-L eliminates this asymmetry. After executing block b , the primary constructs a *hint* H_b containing three components: storage keys with source annotations, account addresses, and bytecode addresses. The primary transmits H_b alongside the block data. The backup uses H_b to prefetch all required state *before* execution begins, eliminating cold misses entirely.

We define the cold-miss barrier formally. Let A_b denote the set of unique storage keys accessed during execution of block b . Without hints, the backup discovers each key in A_b only at the moment it is first referenced, incurring I/O latency on every first access. Because I/O dominates execution time (2.1:1 I/O-to-compute ratio), eliminating these misses through prefetching reduces backup execution time toward the pure-compute lower bound. Section 5 confirms that backup execution closely approaches this bound, achieving a median $24.9\times$ per-block speedup over the baseline.

4.1 Hint Generation

Key Collection. During execution of block b , an EVM inspector intercepts all state-accessing opcodes and records each accessed key into three sets:

- *Storage keys*: $(address, slot)$ pairs from SLOAD and SSTORE.
- *Account addresses*: from BALANCE, SELFBALANCE, EXTCODESIZE, and EXTCODEHASH.
- *Bytecode addresses*: from CALL, STATICCALL, DELEGATECALL, EXTCODECOPY, CREATE, and CREATE2.

Additionally, transaction senders, recipients, and the block beneficiary (coinbase) are added to the account set, since the EVM accesses these accounts implicitly during fee processing and reward distribution. The inspector is lightweight: it reads stack values at each relevant opcode without modifying execution behavior.

Source Annotation. For each storage key (a, k) , the primary determines its *source*, which is a single-byte annotation indicating where the backup should read the value:

- **PlainState** ($\sigma = 0$): The current value resides in the main state table. A single B-tree seek suffices.
- **Zero** ($\sigma = 1$): The slot was never written. The value is zero. No disk I/O is required.
- **Changeset** ($\sigma = 2$): The value must be read from historical change sets. The full two-step lookup is required.

Without source annotations, the backup must perform a two-step lookup for every key: first seeking the history index

Algorithm 1 Ira-L Hint Generation (Primary)

Require: Block $B = \langle T_1, \dots, T_n \rangle$, State database \mathcal{D}
Ensure: Hint set H_B for block B

```

1:  $S \leftarrow \emptyset; A \leftarrow \emptyset; C \leftarrow \emptyset$            // Storage, accounts, code

// Phase 1: Execute and collect accessed keys
2: for  $i \leftarrow 1$  to  $n$  do
3:   Execute  $T_i$  with instrumented EVM
4:    $S \leftarrow S \cup \{(a, k) : T_i$  accesses storage slot  $k$  of account  $a\}$ 
5:    $A \leftarrow A \cup \{a : T_i$  accesses balance or nonce of  $a\}$ 
6:    $C \leftarrow C \cup \{a : T_i$  accesses bytecode of  $a\}$ 

// Phase 2: Annotate storage keys with source information
7: for  $(a, k) \in S$  do
8:    $b^* \leftarrow$  largest  $b < B.num$  where  $(a, k)$  was modified, or  $\perp$ 
9:   if  $b^* = \perp$  then
10:     $src \leftarrow$  ZERO // Slot never written; value is zero
11:   else if  $b^*$  is in pruned history then
12:     $src \leftarrow$  PLAIN // Read from plain state table
13:   else
14:     $src \leftarrow$  HIST // Read from historical changeset
15:    $S[a, k] \leftarrow (a, k, src)$ 

// Phase 3: Serialize and compress
16:  $H_B \leftarrow$  COMPRESS( $S, A, C$ )
17: return  $H_B$ 

```

(a B-tree traversal on a 60-byte composite key, followed by roaring bitmap decompression), then reading the value from the appropriate table. The source annotation eliminates the first step for Plain State keys, reducing two seeks to one and eliminating all I/O for Zero keys. Across our dataset, 46.6% of storage keys resolve to PlainState, 10.5% to Zero, and 43.0% to Changeset (Section C.1). In total, 57.0% of keys bypass the history index entirely, with a per-block median of 55.3%. The source hint removes the confirmation step for PlainState keys and all I/O for Zero keys; only Changeset keys require the full two-step lookup. Section A describes the full history-index lookup algorithm.

Serialization. The hint is serialized in a compact binary format: each storage key requires 53 bytes (20-byte address + 32-byte slot + 1-byte source annotation), and each address key requires 20 bytes. The serialized hint is compressed with Zstandard [26] and stored in a key-value database indexed by block number. Section 5 reports that the median compressed hint is 46.5 KB, achieving a $2.17\times$ compression ratio which is negligible relative to the ~ 2 MB block payload.

Algorithm 1 summarizes the hint generation procedure. The primary executes each transaction with the inspector at-

tached (Phase 1), annotates every storage key with its optimal source (Phase 2), and serializes the result (Phase 3).

4.2 Hint-Based Replay

Sorted Batch Prefetching. Our key algorithmic contribution on the backup side is *sorted batch prefetching*. Upon receiving hints for a batch of blocks, the backup proceeds as follows:

1. Collects all storage keys from the batch into a single sorted collection, ordered lexicographically by *(address, slot)*.
2. Routes keys by source annotation: PlainState keys are read via a single forward cursor walk through the B-tree, converting random I/O into a sequential scan; Zero keys are resolved immediately to zero with no I/O; Changeset keys are deferred to on-demand lookup during execution.
3. Similarly loads account metadata and bytecodes via sorted cursor scans.

Sorting is critical because the underlying database (MDBX, an LMDB-derived B-tree store) stores data in sorted key order. Sorted access maximizes page-cache locality: the cursor advances monotonically through the B-tree, touching each page at most once. Without sorting, each random seek may traverse $O(\log N)$ pages. By batching keys from multiple blocks (default batch size: 32 blocks), the amortized cost per key approaches a single sequential read.

Pipelined Execution. The backup operates in two phases:

- *Phase 1 (warm-up):* Parallel prefetch of approximately 3,000 blocks into an 8 GB in-memory buffer, using a thread pool for initial catch-up.
- *Phase 2 (steady-state):* A dedicated prefetcher thread reads hints and prefetches state in sorted batches, feeding populated caches to the executor through a bounded channel. The executor processes blocks sequentially, consuming prefetched state from the channel. The batch size is tuned so that the next batch completes before the executor finishes the current one, hiding prefetch latency behind execution.

This pipelining ensures that the backup’s wall-clock time is bounded by $\max(\text{prefetch}, \text{execution})$ rather than their sum. Section A provides implementation details of the threading model and channel sizing.

Memory Discipline. Each block’s cache is discarded after execution and there is no cross-block cache. Since hints provide complete coverage for each block, retaining state across blocks is unnecessary. This bounds memory usage to a single block’s working set and avoids the complexity of LRU eviction. As a safety invariant, the cache is backed by a fallback database that panics on any miss: if execution attempts to read a key not provided by the hint, the system halts immediately rather than silently reading from disk. This guarantees that all timing measurements reflect pure cache-hit execution and that any gap in hint coverage is detected at runtime.

Algorithm 2 summarizes the backup replay procedure. The

Algorithm 2 Ira-L Replay (Backup)

Require: Block $B = \langle T_1, \dots, T_n \rangle$, Hints H_B , State database \mathcal{D}

Ensure: Execution matches primary

```

1:  $(S, A, C) \leftarrow \text{DECOMPRESS}(H_B)$ 
2:  $cache \leftarrow \emptyset$ 

// Phase 1: Sort keys for sequential database access
3:  $S' \leftarrow \text{SORTLEXICOGRAPHIC}(S)$  // Sort by  $(a, k)$ 
4:  $A' \leftarrow \text{SORT}(A); C' \leftarrow \text{SORT}(C)$ 

// Phase 2: Prefetch state via sequential cursor traversal
5: for  $a \in A'$  do // Sequential scan
6:    $cache[a] \leftarrow \mathcal{D}.\text{READACCOUNT}(a)$ 

7: for  $(a, k, src) \in S'$  do // Sequential scan
8:   if  $src = \text{ZERO}$  then
9:      $cache[a, k] \leftarrow 0$  // No I/O required
10:   else if  $src = \text{PLAIN}$  then
11:      $cache[a, k] \leftarrow \mathcal{D}.\text{READPLAIN}(a, k)$ 
12:   else
13:      $cache[a, k] \leftarrow \mathcal{D}.\text{READHIST}(a, k, B.\text{num})$ 

14: for  $a \in C'$  do
15:    $cache[a.\text{code}] \leftarrow \mathcal{D}.\text{READBYTECODE}(a)$ 

// Phase 3: Execute from fully-populated cache
16: for  $i \leftarrow 1$  to  $n$  do
17:   Execute  $T_i$  using  $cache$  // All reads hit cache

```

backup decompresses the hint, sorts all keys for sequential access (Phase 1), prefetches state via forward cursor traversal (Phase 2), and executes all transactions from the fully populated cache (Phase 3).

4.3 Correctness and Safety

Hint Completeness. Since we generate hints by instrumenting the actual EVM execution on the primary, they capture exactly the set of keys that will be accessed during replay. The deterministic nature of EVM execution guarantees that the backup, given the same block and state, will access the same keys. The backup’s crash-on-miss database enforces this invariant at runtime: any access to an uncaptured key immediately halts execution, preventing silent divergence.

Advisory Hints. Hints affect only performance, not correctness. If hints are missing, corrupted, or stale, the backup can fall back to standard execution without prefetching, incurring the same I/O cost as the baseline, but producing correct state. This property enables incremental deployment: nodes that do not support hints operate normally, while hint-aware nodes

benefit from faster replay. Incorrect hints may cause degraded performance (cache misses trigger the fallback path) but never produce incorrect state.

State Verification. After executing each block, the primary computes a deterministic hash over all state changes which includes accounts, storage slots, and bytecodes, sorted by key for reproducibility. The backup can optionally verify that its execution produced an identical hash, providing end-to-end correctness checking without requiring full Merkle state root computation.

5 Evaluation

5.1 Configuration

Hardware. Apple M1 Pro (10-core: 8 performance + 2 efficiency), 32 GB unified memory. Benchmarks and trace databases on external 8 TB NVMe SSD (Sabrent, USB enclosure).

Software. Rust 1.88 (edition 2024), Python 3.14 with matplotlib 3.10, numpy 2.4. Apache Parquet (Arrow 54) with Zstandard compression for trace storage. reth (commit 62abfdae) for trace collection (requires synced Ethereum mainnet node).

Methodology. We evaluate Ira-L using the same two-week dataset of 100,800 consecutive Ethereum mainnet blocks (blocks 24,019,447–24,120,246). All benchmarks start with a cold OS page cache (purged before each run) to measure worst-case I/O performance. We compare four configurations:

- *Baseline*: unmodified reth executing blocks sequentially.
- *Primary*: reth with hint generation enabled.
- *Backup (sequential)*: backup replaying with hints using a single prefetch thread.
- *Backup (parallel- k)*: backup replaying with k concurrent prefetch threads ($k \in \{16, 64\}$).

5.2 Hint Overhead on Primary

The primary generates hints during normal block execution. We measure two components of overhead: *hint construction* (building the next-access map) and *hint serialization* (compressing and writing hints to disk). We compare against the unmodified baseline to quantify the total cost.

Wall-Time Overhead. Table 3 summarizes the end-to-end wall-time comparison. The baseline executes all 100,800 blocks in 23,250 s, while the primary completes in 29,889 s which is a 28.6% increase in wall time. This overhead reflects not only hint generation but also any secondary effects of instrumentation on execution (e.g., additional memory pressure, cache interference).

Per-Block Hint Cost. To isolate the direct cost of hint generation, we examine the per-block breakdown of hint construction and serialization time as a fraction of execution time (Figure 9). Across all blocks, hint construction consumes 940

Table 3: Wall-time comparison between baseline and primary.

Configuration	Wall Time (s)	Overhead
Baseline	23,250	—
Primary (with hints)	29,889	28.6%

s and hint serialization 778 s, totaling 1,719 s of hint-related work, which is 10.9% of the aggregate execution time 15,717 s. The median per-block hint fraction is 12.1%, with a 95th-percentile value of 22.1%.

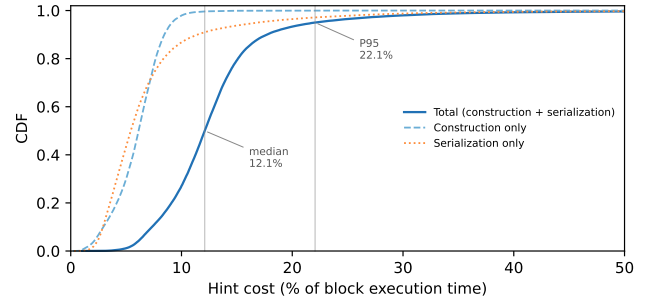


Figure 9: CDF of per-block hint cost as a percentage of block execution time. Construction and serialization each contribute roughly half the total overhead, with a median of 12.1% and a 95th percentile of 22.1%.

Figure 10 shows how each component scales with block size. Construction time grows linearly with the number of unique storage keys ($r = 0.79$) at approximately $8.1 \mu\text{s}$ per key, reflecting the per-key history index query. Serialization time, by contrast, is nearly independent of block size ($r = 0.03$) and clusters tightly around 12.5 ms (IQR 11.9–13.1 ms), dominated by the fixed cost of flushing the database write transaction. The per-block hint fraction therefore varies primarily because *execution time* varies which is driven by I/O and page cache state, not because hint cost itself is unpredictable. A detailed variance decomposition is provided in Section C.3.

These per-block fractions (median 12.1%, P95 22.1%) reflect a conservative, fully sequential measurement where hint construction and serialization run inline with block execution. In practice, both components are independent of execution correctness and can be overlapped with the next block’s processing. Hint construction (6.0% of aggregate execution time) builds a map from keys already collected during EVM execution and queries the storage history index to annotate each key with its optimal read source (Section A). Hint serialization (5.0%) compresses and persists the hint to disk, requiring no executor state at all. Production reth already employs a multi-threaded architecture with a dedicated executor thread pool and a separate storage writer thread (Section A); in this model,

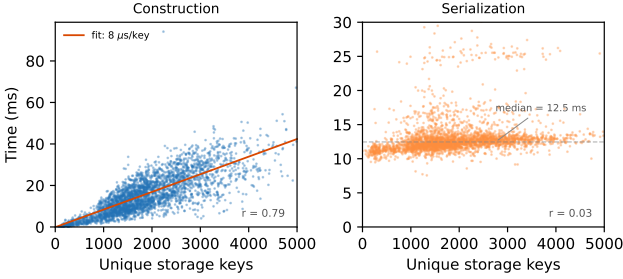


Figure 10: Hint cost scaling with block working set size. Construction time (left) scales linearly with the number of unique storage keys ($r = 0.79$, $\sim 8.1 \mu$ s/key). Serialization time (right) is nearly constant regardless of block size ($r = 0.03$, median 12.5 ms).

hint construction can execute on the existing thread pool and serialization can run on the storage thread, overlapping both with the next block’s execution. Under such pipelining, the effective overhead approaches zero for all but the final block in a batch. Moreover, the cost is paid once by the primary and recovered on every backup: even with sequential prefetching, the backup replays $5.2\times$ faster in wall time (Section 5.3), yielding a net system-wide speedup despite the primary’s 28.6% wall-time increase.

Hint Sizes. Figure 11 shows the distribution of per-block hint sizes. The median compressed hint is 46.5 KB (mean 51.5 KB), with a 95th-percentile of 104.2 KB and a maximum of 239.0 KB. Zstandard compression achieves a $2.17\times$ reduction from the raw representation (median 102.2 KB raw). Figure 12 confirms that these sizes remain stable across the entire 100,800-block range, with no visible trend or drift.

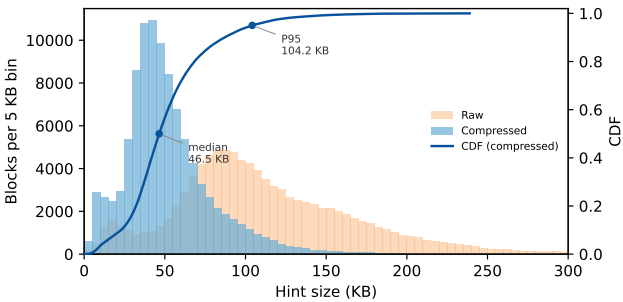


Figure 11: Distribution of per-block hint sizes. Histogram bins show block counts for raw (orange) and compressed (blue) sizes; the overlaid CDF (dark blue) marks the median (46.5 KB) and P95 (104.2 KB) of compressed hints.

A hint contains one fixed-size entry per unique storage key accessed in the block, encoding the key hash and its optimal read source. The raw hint size is therefore determined

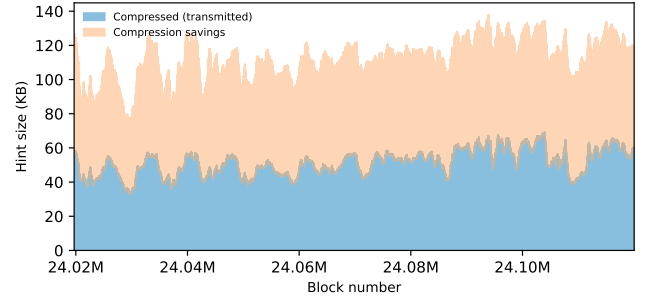


Figure 12: Hint sizes across blocks (500-block rolling average). The bottom layer shows the compressed size transmitted to backups; the top layer shows the bytes eliminated by Zstandard compression.

entirely by the key count: a block touching 1,806 unique keys (the median; Section 3) produces a hint of 102.2 KB before compression. Zstandard is effective because, while the key hashes themselves are high-entropy, the accompanying metadata fields (source flags, offsets) are highly regular.

These hint sizes are negligible relative to the block data they accompany (~ 2 MB per block): even the 95th-percentile compressed hint adds only $\sim 5\%$ to the block payload. On a 1 Gbps link, transmitting the P95 hint takes under 1 ms which is orders of magnitude less than the replay time saved. Hint size is also bounded by the EVM gas limit, which caps the number of storage operations per block. In practice, hints grow only when blocks are large, and large blocks are precisely those where replay savings are greatest (Section 5.3).

5.3 Backup Speedup

We now evaluate how effectively hints accelerate backup replay. For each block, the backup reads the hint, prefetches the indicated keys into its MDBX cache, and then executes the block. We report the per-block speedup as speedup = $t_{\text{baseline}} / (t_{\text{wait}} + t_{\text{exec}})$, where t_{baseline} is the baseline execution time, t_{wait} is the time the executor stalls waiting for prefetch, and t_{exec} is the backup’s execution time.

5.3.1 Per-Block Speedup Distribution

Figure 13 shows per-block speedup across the entire block range for the sequential backup configuration; Table 10 in the appendix lists the key percentiles for all three configurations.

The backup achieves a median speedup of $24.9\times$ (mean $28.9\times$) across the sequential configuration, with the parallel configurations yielding nearly identical distributions. In terms of aggregate wall time, the sequential backup completes all 100,800 blocks in 4,366 s ($5.2\times$ faster than the baseline’s 22,604 s), parallel-16 in 956 s ($23.6\times$), and parallel-64 in 871 s ($25.9\times$).

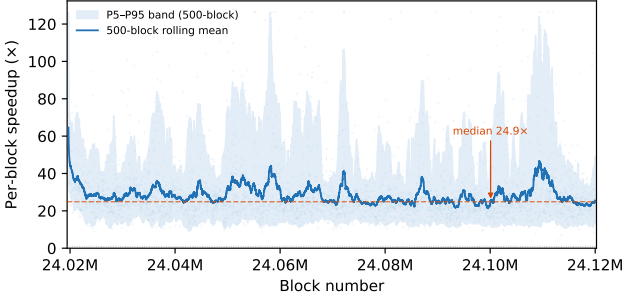


Figure 13: Per-block speedup (sequential backup vs. baseline) across 100,800 blocks. Each point is one block; the solid line shows a 500-block rolling average and the shaded band spans the P5–P95 range. The dashed line marks the median speedup.

The speedup magnitude follows directly from Amdahl’s law and the I/O-dominance of the baseline. Using backup execution time as a proxy for pure compute (the backup’s cache is warm from prefetching), the baseline spends approximately 96% of its time on page faults and only $\sim 4\%$ on EVM computation. Eliminating all I/O yields a theoretical ceiling of $1/(1 - 0.96) = 25\times$ which is almost exactly the observed median. Hint-driven prefetching approaches this ceiling because it resolves *every* storage key before execution begins, converting the baseline’s serial page faults into a single overlapped prefetch phase.

Figure 13 reveals three regimes. First, an *initial transient* in the first ~ 500 blocks where speedup exceeds $50\times$: the baseline starts with a fully cold OS page cache and mean execution time of 570 ms, while the backup begins against an already-populated MDBX file and has zero wait time, completing in under 9 ms. As the baseline’s page cache fills (RSS grows from 0.2 GB to ~ 8 GB over this window), its execution time drops and the speedup converges to steady state.

Second, the *steady-state* regime (blocks 1,000+) exhibits a stable rolling mean of 27-30 \times with no meaningful drift and dividing the trace into 10 equal segments yields segment means that vary by less than $\pm 10\%$ of the overall mean. This stability confirms that the speedup is determined by the per-block I/O fraction rather than transient cache effects.

Third, *periodic bursts* of 60-130 \times appear throughout the trace. These high-speedup blocks have 2 \times higher baseline execution time (more page cache misses) and 38% more unique storage keys than the median, yet complete with zero backup wait time. The bursts are not sustained, the median cluster length is 1 block. This indicates that they arise from individual blocks whose working sets happen to miss heavily in the baseline’s page cache.

5.3.2 Tail Behavior

While the median speedup is substantial, we examine the fraction of blocks where the backup is *slower* than the baseline (Table 11 in the appendix).

With sequential prefetching, 3.02% of blocks experience a regression (Table 11 in the appendix). The root cause is MDBX’s use of memory-mapped I/O: each cold page access blocks the faulting thread until the kernel completes the read (Section A.3), so a single prefetch thread issues at most one storage I/O at a time. When a block touches thousands of uncached B-tree pages, this serialization causes the executor to stall waiting for prefetch to finish, negating the I/O savings. Among these regressed blocks, the median speedup is $0.18\times$ ($5.5\times$ slower than baseline), with a mean of $0.20\times$ ($4.9\times$ slower). At 64 prefetch threads, only 0.09% of blocks remain slower than the baseline.

5.3.3 Wait Time Analysis

Figure 14 decomposes aggregate wall time by whether the executor stalled waiting for prefetch to complete.

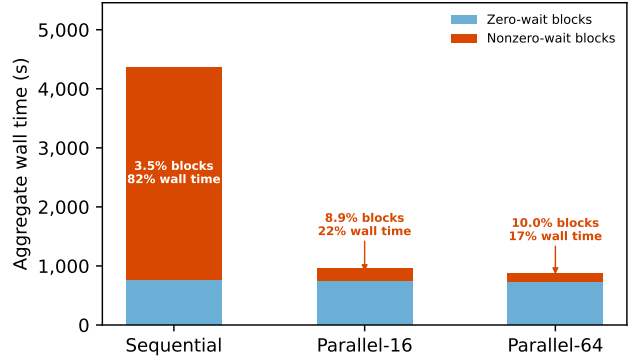


Figure 14: Aggregate wall time decomposed by executor wait. For each configuration, the bottom segment is wall time from blocks with zero wait; the top segment is from blocks where the executor stalled for prefetch.

With sequential prefetching, 96.5% of blocks complete with zero wait time, yet the remaining 3.5% blocks, which are the same large-working-set blocks identified in Section 5.3.2, account for over 80% of aggregate wall time. Parallel prefetching eliminates these stalls: with multiple threads, page faults are in flight simultaneously and the prefetch phase completes before the executor is ready to begin. This reduction in wait time is the primary driver of the wall-time improvement from sequential to parallel configurations, as execution time itself is unchanged.

5.4 Thread Scaling

Figure 15 shows the wall-time speedup relative to the baseline as a function of prefetch thread count across ten configurations (1–64 threads). The curve exhibits three regimes. First, a *steep scaling* region from 1 to 8 threads where wall time drops from 4,366 s to \sim 1,088 s ($4\times$ reduction), reflecting near-linear conversion of serial page faults into parallel I/O. Second, a *diminishing-returns* region from 8 to 16 threads where wall time falls further to 957 s ($4.6\times$ over sequential) as the SSD’s command queue approaches saturation. Third, a *plateau* beyond 16 threads: doubling from 16 to 32 yields only a 7% reduction, and quadrupling to 64 threads reaches 871 s ($1.1\times$ over 16 threads), indicating that the I/O bandwidth of our NVMe SSD is fully saturated.

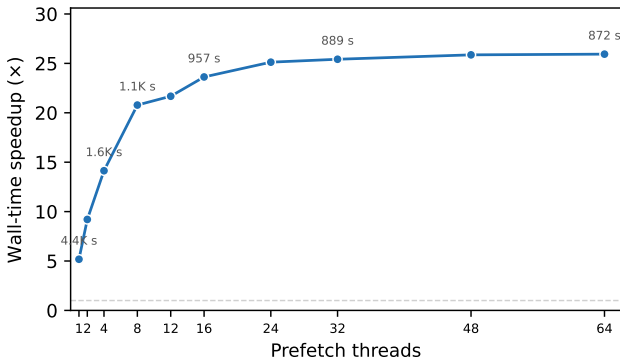


Figure 15: Wall-time speedup relative to the baseline as a function of prefetch thread count (1–64 threads). Labels show absolute wall time. The curve saturates around 8–16 threads, consistent with I/O bandwidth limits of the NVMe SSD.

The steep initial gains reflect the conversion of serial page faults into parallel I/O: when a single thread prefetches sequentially, each MDBX page fault blocks until the SSD services the request. With multiple concurrent threads, page faults are in flight simultaneously, saturating the SSD’s queue depth and achieving higher throughput. The knee at 8–16 threads corresponds to the device’s maximum queue depth being reached; additional threads merely compete for the same bandwidth. The optimal thread count is hardware-dependent since systems with higher-bandwidth storage (e.g., PCIe 5.0 NVMe, RAID arrays) may shift the knee to higher thread counts.

5.5 Resource Usage

A key property of Ira-L is that hint-based prefetching does not require additional memory beyond what the baseline already uses. Table 4 shows the peak resident set size (RSS) for each configuration.

Table 4: Peak resident set size across configurations.

Configuration	Peak RSS (GB)
Baseline	26.3
Primary	26.1
Backup	26.0

All three configurations consume comparable memory (\sim 26.3 GB), dominated by the MDBX memory-mapped database. The primary’s hint data structures (the next-access map) add negligible overhead: the map contains at most one entry per unique key in the current block (median 1,806 keys), each requiring a few tens of bytes, totaling at most a few hundred kilobytes per block.

The backup’s prefetch threads share the same memory-mapped file and do not allocate additional buffers. They simply trigger page faults that the OS services into the existing page cache. This design ensures that Ira-L’s memory footprint is determined by the database size, not by the hint mechanism.

6 Discussion

Application scope. Our framework has applications beyond Ethereum. The key requirements for Ira to be applicable in a distributed database system are: (i) primary-backup architecture, i.e., there exists a node that executes first and the others follow, (ii) replay is storage-bound, where I/O is a bottleneck, and (iii) the execution is deterministic. Systems such as the following potentially benefit from our solution:

1. *Replicated databases*, e.g., MySQL Group Replication [11], MariaDB Galera [3], PostgreSQL streaming replication [1], CockroachDB [58], TiDB [34], and deterministic databases like Calvin [59], use primary-backup architecture to deterministically replay database operations. All of them have nodes with complete execution traces that can assist replicas during replication.
2. *Distributed key-value stores*, e.g., FoundationDB [70], use consensus-based replication where followers replay the primary’s logs. For stores with large state that exceeds memory, hints can naturally encode access patterns to improve performance.
3. *Blockchain systems* such as Solana [66], Sui [14], Aptos [2, 32], Cosmos [4, 23], and the Hyperledger family [18] have validators that propose blocks while other nodes replay using a VM layer, and are strong candidates for Ira’s hint-based acceleration.

Deployment considerations. *Layer-1 optional.* Existing database systems can deploy Ira without enforcing hint correctness as part of the underlying synchronization protocol.

Blockchains that implement this need not enforce correctness as part of the block proposal mechanism as the hints are advisory and affect only performance.

Incentive Mechanisms. We can incentivize our system with rewards. Today, Ethereum incentivizes transactions that provide an access list (a list of accounts accessed by the transaction) with discounted gas costs. If the access list is wrong, the user pays more gas. A similar mechanism can ensure that block producers generate correct hints.

Security considerations. Our hint generation does not rely on the primary being non-faulty. On omission of hints, nodes can simply revert to a backup caching mechanism such as LRU. We take great care in designing the hints so that a malicious hint only increases the latency of computation but does not affect the correctness of the underlying protocol. However, systems operating under stronger trust models, e.g., those using a Trusted Execution Environment (TEE) or crash-fault models, can take advantage of the non-faulty primary and provide additional hints that can further speed up verification as well as replay. Note that hints reveal access patterns, which may be a privacy consideration in permissioned blockchains where transaction contents are confidential.

Limitations and future work. Our implementation targets a single-threaded execution model. Concurrent execution would require coordination for hint data structures, potentially through partitioning hints by key ranges, usage of synchronization primitives and barriers. Notably, Ira can also assist concurrent execution with hints that aid in improving concurrent replay. We can extend the hints to support parallel replay across multiple threads and explore partitioned hint structures to avoid synchronization overheads. Another limitation of our work is that it assumes the replay workload is storage-bound. Compute-bound replay can be optimized using hints that support improved concurrency, but this remains future work. Beyond cache eviction, hints could guide write batching, memory allocation, and as already stated, concurrency to further accelerate replay.

7 Related Work

Optimal Cache Replacement. Belady’s MIN algorithm [20], proved optimal by Mattson et al. [45], provides optimal offline cache replacement by evicting the item whose next access is furthest in the future. Some works use adaptive heuristics, e.g., the *adaptive replacement cache* [46] (ARC) and LIRS [38] which use heuristics to dynamically balance between recency and frequency, and LeCaR [62] uses regret minimization to learn this balance online. Another approach is to use hardware prefetchers which predict future accesses to hide memory latency. Prefetch-aware replacement policies like PACMan [65] and SHiP [64] adjust eviction priorities for prefetched blocks. A different approach is to approximate the MIN algorithm from history. Works such as the HawkEye cache by Jain and Lin [37] observe that MIN minimizes *total*

misses but not *demand* misses in the presence of prefetching. They introduce Demand-MIN and Flex-MIN to navigate this tradeoff. The Hawkeye cache [36] uses past access patterns to approximate MIN decisions. Subsequent works like Mockingjay [55] and Glider [56] use machine learning to improve prediction accuracy but require specialized hardware structures and still cannot exceed the accuracy ceiling imposed by predicting from past behavior alone. Recent deep learning approaches [30, 57, 68] use neural networks to learn access patterns, achieving higher accuracy than traditional heuristics but remaining fundamentally limited to inference from history. Our work differs from these works in that we transmit exact future access information from primary to backup, enabling true optimal eviction without prediction.

Hint-based systems. Mowry et al. [49] presented the pioneering work with the idea of using compiler based automation to optimize prefetching. The TIP system [52] by Patterson et al. was one of the early works proposing the *hint-based* paradigm where the applications advise the OS with *advisory hints* to improve prefetching and caching optimizations. HintStor [31] presents a framework to propagate I/O hints across the storage stack in heterogeneous storage systems. Mandal et al. [44] demonstrate hints at the block layer of storage for deduplication, where applications mark unique writes (NODEDUP) and prefetch requests (PREFETCH) to avoid redundant hash computations. Modern OS provide system calls such as madvise [10] and fadvise [13] where applications can advise the OS on the access pattern such as random, sequential, will-need, and don’t need. Database systems such as Oracle’s INDEX and USE_NL hints allow developers to override the query planner run before executing a query. These approaches share the limitation that hints are *manually* specified and require domain knowledge, or *statically derived* which are limited to predictable patterns like loops. In contrast, our framework Ira generates hints automatically from the primary’s execution trace, providing complete and exact future access information without programmer effort.

Replay in Replicated Databases. Modern databases build on ARIES-style write-ahead logging [48], which established the three-phase recovery protocol (analysis, redo, undo) now used across the industry [47]. In primary-backup replication, backups continuously replay the primary’s log to maintain synchronized state. Deterministic databases such as Calvin [59] and Aria [43] ensure replicas converge to identical states by replaying transaction logs in a deterministic order without coordination. A key challenge is the *parallelism gap*: primaries execute transactions concurrently, but backups traditionally replay logs serially. KuaFu [25] addresses this by tracking dependencies to enable parallel replay, demonstrating that serial replay sustains less than one-third of primary throughput thus underscoring the need for systems such as Ira. Cloud-native databases have further evolved replay architectures: Amazon Aurora [61] pushes redo log application to a distributed storage tier, treating the log as the database itself,

while Socrates [19] (Azure SQL Hyperscale) uses a four-tier architecture with dedicated Page Servers for log application. PolarDB-SCC [67] tackles the consistency challenges arising from asynchronous log propagation to read-only replicas. While these works focus on replay correctness, parallelism, or architectural placement of log application, none optimize *cache eviction decisions* during replay. Ira is complementary: it accelerates replay within any of these architectures by exploiting the primary’s knowledge of future accesses to achieve Belady-optimal caching.

Blockchain State Synchronization. Blockchain nodes face significant replay challenges during both initial synchronization and ongoing block validation. Early Ethereum clients performed full sync by re-executing every transaction from genesis, but this approach became impractical as chain history grew. Geth [16] introduced fast sync [6] (2015) and later snap sync [7] (2021), which download recent state directly and reconstruct the Merkle trie locally, achieving 10× faster initial sync. Erigon [15] (formerly Turbo-Geth) pioneered *staged sync* [5], a pipelined architecture that processes headers, bodies, senders recovery, and execution as discrete stages; Reth [12] adopts this architecture in Rust for further performance gains. Despite these optimizations, the execution stage, where transactions are replayed to compute state, remains the primary bottleneck and cannot be parallelized within staged sync. To enable parallel validation, some systems require transactions to declare their data dependencies upfront. Ethereum’s EIP-2930 [53] introduced optional access lists that pre-declare storage slots, though adoption remains low: analysis shows only 1.46% of transactions include access lists despite 42.6% benefiting from them [33]. Solana’s Sealevel runtime [66] mandates read/write set declarations, enabling lock-based parallel execution across non-conflicting transactions. For systems without mandatory access declarations, Block-STM [32] provides optimistic parallel execution using software transactional memory techniques, achieving 170k transactions per second on Aptos. Sui [22] takes an object-centric approach where owned objects bypass consensus entirely, enabling sub-second finality for non-shared state. Forerunner [24] exploits the time window between transaction dissemination and consensus to speculatively pre-execute transactions, achieving 10× speedup through constraint-based multi-trace specialization. Looking forward, Verkle trees [41] promise to enable stateless clients by reducing witness sizes from ~ 150 KB to 1 – 2 KB, allowing validators to verify blocks without storing full state. While these works optimize sync architecture, transaction scheduling, or state representation, none address *cache eviction* during replay. Our system Ira is the first complementary approach that provides exact future access information, enabling Belady-optimal caching during the execution stage improving upon the bottleneck that staged sync, access lists, and parallel execution engines aimed to solve.

Speculative and parallel execution. Parallel transaction ex-

ecution has been extensively studied in both database and blockchain contexts. Kung and Robinson’s seminal work on optimistic concurrency control (OCC) [40] established the read-validate-write paradigm that underlies modern parallel execution systems. Silo [60] demonstrated that OCC can achieve nearly 700,000 transactions per second on multi-core hardware by eliminating centralized contention points. For workloads with high contention on popular records, Doppe [50] introduced phase reconciliation, cycling between split phases (where commutative operations execute on per-core state) and joined phases (where results are merged), achieving up to 38× higher throughput than conventional protocols. Deterministic approaches like BOHM [27] pre-compute transaction dependencies to enable parallel execution without runtime conflict detection, while PWV [28] increases concurrency by making writes visible before transaction commit through piece-wise execution. In the blockchain space, the previous paragraph discussed systems like Block-STM, Forerunner, and access-list-based parallelization; commercial efforts such as Monad [8] and Sei [17] further pursue optimistic parallel EVM execution. These works share a common goal: maximizing transaction throughput by exploiting parallelism. Ira is orthogonal to and composable with all of these approaches. Even when transactions execute in parallel, each execution thread must still manage its cache and make eviction decisions. By providing exact future access information, Ira enables Belady-optimal caching *within* each parallel execution context, reducing I/O latency regardless of the concurrency control protocol employed.

8 Conclusion

We presented Ira, a general framework for accelerating backup replay in primary-backup replication by transmitting compact hints that encode the primary’s knowledge of future access patterns. The framework applies to any storage-bound, deterministic primary-backup system including replicated databases, distributed key-value stores, and blockchain platforms. We demonstrated its practicality through Ira-L, a concrete instantiation for Ethereum block synchronization implemented in the production client reth, showing significant replay speedups at low hint overheads.

References

- [1] 26.2. Log-Shipping Standby Servers.
- [2] The Aptos Blockchain: Safe, Scalable, and Upgradeable Web3 Infrastructure.
- [3] Certification-Based Replication | Galera Cluster | MariaDB Documentation.
- [4] Cosmos Stack Developer Documentation.

- [5] [Erigon/eth/stagedsync/README.md](https://github.com/Erigon/eth/stagedsync/README.md) at release/2.60 · erigontech/erigon.
- [6] [Eth/63 fast synchronization algorithm by karalabe · Pull Request #1889 · ethereum/go-ethereum.](https://github.com/ethereum/go-ethereum/pull/1889)
- [7] [Geth v1.10.0.](https://geth.ethereum.org/docs/installation/installing-geth)
- [8] [Introduction | Monad Developer Documentation.](https://monad.readthedocs.io/en/latest/introduction.html)
- [9] [Libmdbx: One of the fastest embeddable key-value engine.](https://libmdbx.readthedocs.io/en/latest/introduction.html)
- [10] [Madvise\(2\) - Linux manual page.](https://man7.org/linux/man-pages/man2/madvise.2.html)
- [11] [MySQL :: MySQL 8.0 Reference Manual :: 20 Group Replication.](https://dev.mysql.com/doc/refman/8.0/en/group-replication.html)
- [12] [Paradigmxyz/reth.](https://paradigmxyz.github.io/reth/)
- [13] [Posix_fadvise\(2\) - Linux manual page.](https://man7.org/linux/man-pages/man2/posix_fadvise.2.html)
- [14] [The Sui Smart Contracts Platform.](https://sui.io/docs/learn/smart-contracts)
- [15] [Erigontech/erigon. Erigon, January 2026.](https://erigon.tech/)
- [16] [Ethereum/go-ethereum. ethereum, January 2026.](https://ethereum.org/en/developer/apis/json-rpc/)
- [17] [Sei Parallelization Engine: Multi-core Blockchain Execution | Sei Docs, January 2026.](https://sei.io/docs/learn/parallelization-engine)
- [18] [Elli Androulaki, Artem Barger, Vita Bortnikov, Christian Cachin, Konstantinos Christidis, Angelo De Caro, David Enyeart, Christopher Ferris, Gennady Laventman, Yacov Manovich, Srinivasan Muralidharan, Chet Murthy, Binh Nguyen, Manish Sethi, Gari Singh, Keith Smith, Alessandro Sorniotti, Chrysoula Stathakopoulou, Marko Vukolić, Sharon Weed Cocco, and Jason Yellick. Hyperledger Fabric: A Distributed Operating System for Permissioned Blockchains. In *Proceedings of the Thirteenth EuroSys Conference*, pages 1–15.](https://www.usenix.org/conference/13eurosys/presentation/androulaki)
- [19] [Panagiotis Antonopoulos, Alex Budovski, Cristian Diaconu, Alejandro Hernandez Saenz, Jack Hu, Hanuma Kodavalla, Donald Kossmann, Sandeep Lingam, Umar Farooq Minhas, Naveen Prakash, Vijendra Purohit, Hugh Qu, Chaitanya Sreenivas Ravella, Krystyna Reisteter, Sheetal Shrotri, Dixin Tang, and Vikram Wakade. Socrates: The New SQL Server in the Cloud. In *Proceedings of the 2019 International Conference on Management of Data*, SIGMOD ’19, pages 1743–1756, New York, NY, USA, June 2019. Association for Computing Machinery.](https://www.usenix.org/conference/sigmod19/presentation/antonopoulos)
- [20] [L. A. Belady. A study of replacement algorithms for a virtual-storage computer. 5\(2\):78–101.](https://www.jstor.org/stable/20033100)
- [21] [Christopher Berner. Cberner/redb, January 2026.](https://github.com/ChristopherBerner/cberner/redb)
- [22] [Sam Blackshear, Andrey Chursin, George Danezis, Anastasios Kichidis, Lefteris Kokoris-Kogias, Xun Li, Mark Logan, Ashok Menon, Todd Nowacki, Alberto Sonnino, Brandon Williams, and Lu Zhang. Sui Lutris: A Blockchain Combining Broadcast and Consensus, October 2024.](https://www.usenix.org/conference/24blockchain/presentation/blackshear)
- [23] [Ethan Buchman, Jae Kwon, and Zarko Milosevic. The latest gossip on BFT consensus.](https://www.usenix.org/conference/21sosp/presentation/buchman)
- [24] [Yang Chen, Zhongxin Guo, Runhuai Li, Shuo Chen, Lidong Zhou, Yajin Zhou, and Xian Zhang. Forerunner: Constraint-based Speculative Transaction Execution for Ethereum. In *Proceedings of the ACM SIGOPS 28th Symposium on Operating Systems Principles*, SOSP ’21, pages 570–587, New York, NY, USA, October 2021. Association for Computing Machinery.](https://www.usenix.org/conference/21sosp/presentation/chen)
- [25] [Chuntao Hong, Dong Zhou, Mao Yang, Carbo Kuo, Lin-tao Zhang, and Lidong Zhou. KuaFu: Closing the parallelism gap in database replication. In *2013 IEEE 29th International Conference on Data Engineering \(ICDE\)*, pages 1186–1195. IEEE.](https://www.usenix.org/conference/13icde/presentation/hong)
- [26] [Facebook. Zstandard - Real-time data compression algorithm.](https://facebook.zstandard.net/)
- [27] [Jose M. Faleiro and Daniel J. Abadi. Rethinking serializable multiversion concurrency control, December 2015.](https://www.usenix.org/conference/15osdi/presentation/faleiro)
- [28] [Jose M. Faleiro, Daniel J. Abadi, and Joseph M. Hellerstein. High performance transactions via early write visibility. *Proceedings of the VLDB Endowment*, 10\(5\):613–624, January 2017.](https://www.usenix.org/conference/17vldb/presentation/faleiro)
- [29] [Apache Software Foundation. Apache Parquet.](https://www.apache.org/foundation/paper-parquet.html)
- [30] [Gaddisa Olani Ganfure, Chun-Feng Wu, Yuan-Hao Chang, and Wei-Kuan Shih. DeepPrefetcher: A Deep Learning Framework for Data Prefetching in Flash Storage Devices. 39\(11\):3311–3322.](https://www.usenix.org/conference/15icde/presentation/gaddisa)
- [31] [Xiongzi Ge, Zhichao Cao, David H. C. Du, Pradeep Ganesan, and Dennis Hahn. HintStor: A Framework to Study I/O Hints in Heterogeneous Storage. 18\(2\):18:1–18:24.](https://www.usenix.org/conference/18osdi/presentation/ge)
- [32] [Rati Gelashvili, Alexander Spiegelman, Zhuolun Xiang, George Danezis, Zekun Li, Yu Xia, Runtian Zhou, and Dahlia Malkhi. Block-STM: Scaling Blockchain Execution by Turning Ordering Curse to a Performance Blessing.](https://www.usenix.org/conference/20blockchain/presentation/gelashvili)
- [33] [Lioba Heimbach, Quentin Kniep, Yann Vonlanthen, Roger Wattenhofer, and Patrick Züst. Dissecting the EIP-2930 Optional Access Lists, December 2023.](https://www.usenix.org/conference/23osdi/presentation/heimbach)

[34] Dongxu Huang, Qi Liu, Qiu Cui, Zhuhe Fang, Xiaoyu Ma, Fei Xu, Li Shen, Liu Tang, Yuxing Zhou, Menglong Huang, Wan Wei, Cong Liu, Jian Zhang, Jianjun Li, Xuelian Wu, Lingyu Song, Ruoxi Sun, Shuaipeng Yu, Lei Zhao, Nicholas Cameron, Liquan Pei, and Xin Tang. TiDB: A Raft-based HTAP database. *Proceedings of the VLDB Endowment*, 13(12):3072–3084, August 2020.

[35] Patrick Hunt, Mahadev Konar, Flavio P. Junqueira, and Benjamin Reed. ZooKeeper: Wait-free coordination for internet-scale systems. In *Proceedings of the 2010 USENIX Conference on USENIX Annual Technical Conference*, USENIXATC’10, page 11. USENIX Association.

[36] Akanksha Jain and Calvin Lin. Back to the future: Leveraging Belady’s algorithm for improved cache replacement. 44(3):78–89.

[37] Akanksha Jain and Calvin Lin. Rethinking Belady’s Algorithm to Accommodate Prefetching. In *2018 ACM/IEEE 45th Annual International Symposium on Computer Architecture (ISCA)*, pages 110–123.

[38] Song Jiang and Xiaodong Zhang. LIRS: An efficient low inter-reference recency set replacement policy to improve buffer cache performance. 30(1):31–42.

[39] Flavio P. Junqueira, Benjamin C. Reed, and Marco Serafini. Zab: High-performance broadcast for primary-backup systems. In *Proceedings of the 2011 IEEE/IFIP 41st International Conference on Dependable Systems&Networks*, DSN ’11, pages 245–256. IEEE Computer Society.

[40] H. T. Kung and John T. Robinson. On optimistic methods for concurrency control. *ACM Transactions on Database Systems*, 6(2):213–226, June 1981.

[41] John Kuszmaul. Verkle Trees, 2018.

[42] Leslie Lamport. Paxos made simple. pages 51–58.

[43] Yi Lu, Xiangyao Yu, Lei Cao, and Samuel Madden. Aria: A fast and practical deterministic OLTP database. *Proceedings of the VLDB Endowment*, 13(12):2047–2060, August 2020.

[44] Sonam Mandal, Geoff Kuenning, Dongju Ok, Varun Shastry, Philip Shilane, Sun Zhen, Vasily Tarasov, and Erez Zadok. Using Hints to Improve Inline Block-layer Deduplication. pages 315–322.

[45] R.L. Mattson, J. Gecsei, D. R. Slutz, and I. L. Traiger. Evaluation techniques for storage hierarchies. 9(2):78–117.

[46] Nimrod Megiddo and Dharmendra S. Modha. {ARC}: A {Self-Tuning}, Low Overhead Replacement Cache.

[47] C Mohan. Repeating History Beyond ARIES. *VLDB*, 99:7–10, September 1999.

[48] C. Mohan, Don Haderle, Bruce Lindsay, Hamid Pirahesh, and Peter Schwarz. ARIES: A transaction recovery method supporting fine-granularity locking and partial rollbacks using write-ahead logging. *ACM Trans. Database Syst.*, 17(1):94–162, March 1992.

[49] Todd C. Mowry, Monica S. Lam, and Anoop Gupta. Design and evaluation of a compiler algorithm for prefetching. 27(9):62–73.

[50] Neha Narula, Cody Cutler, Eddie Kohler, and Robert Morris. Phase Reconciliation for Contended In-Memory Transactions. In *11th USENIX Symposium on Operating Systems Design and Implementation (OSDI 14)*, pages 511–524, 2014.

[51] Diego Ongaro and John Ousterhout. In Search of an Understandable Consensus Algorithm. *Proceedings of USENIX ATC ’14: 2014 USENIX Annual Technical Conference.*, June 2014.

[52] R. H. Patterson, G. A. Gibson, E. Ginting, D. Stodolsky, and J. Zelenka. Informed prefetching and caching. In *Proceedings of the Fifteenth ACM Symposium on Operating Systems Principles*, SOSP ’95, pages 79–95. Association for Computing Machinery.

[53] Ethereum Improvement Proposals. EIP-2930: Optional access lists.

[54] Fred B Schneider. Implementing fault-tolerant services using the state machine approach: A tutorial. *ACM Computing Surveys*, 22(4):299–319, December 1990.

[55] Ishan Shah, Akanksha Jain, and Calvin Lin. Effective Mimicry of Belady’s MIN Policy. In *2022 IEEE International Symposium on High-Performance Computer Architecture (HPCA)*, pages 558–572.

[56] Zhan Shi, Xiangru Huang, Akanksha Jain, and Calvin Lin. Applying Deep Learning to the Cache Replacement Problem. In *Proceedings of the 52nd Annual IEEE/ACM International Symposium on Microarchitecture*, MICRO-52, pages 413–425. Association for Computing Machinery.

[57] Zhan Shi, Akanksha Jain, Kevin Swersky, Milad Hashemi, Parthasarathy Ranganathan, and Calvin Lin. A hierarchical neural model of data prefetching. In *Proceedings of the 26th ACM International Conference on Architectural Support for Programming Languages and Operating Systems*, ASPLOS ’21, pages 861–873. Association for Computing Machinery.

[58] Rebecca Taft, Irfan Sharif, Andrei Matei, Nathan Van-Benschoten, Jordan Lewis, Tobias Grieger, Kai Niemi, Andy Woods, Anne Birzin, Raphael Poss, Paul Bardea, Amruta Ranade, Ben Darnell, Bram Gruneir, Justin Jaffray, Lucy Zhang, and Peter Mattis. CockroachDB: The Resilient Geo-Distributed SQL Database. In *Proceedings of the 2020 ACM SIGMOD International Conference on Management of Data*, SIGMOD ’20, pages 1493–1509. Association for Computing Machinery.

[59] Alexander Thomson, Thaddeus Diamond, Shu-Chun Weng, Kun Ren, Philip Shao, and Daniel J. Abadi. Calvin: Fast distributed transactions for partitioned database systems. In *Proceedings of the 2012 ACM SIGMOD International Conference on Management of Data*, SIGMOD ’12, pages 1–12. Association for Computing Machinery.

[60] Stephen Tu, Wenting Zheng, Eddie Kohler, Barbara Liskov, and Samuel Madden. Speedy transactions in multicore in-memory databases. In *Proceedings of the Twenty-Fourth ACM Symposium on Operating Systems Principles*, SOSP ’13, pages 18–32, New York, NY, USA, November 2013. Association for Computing Machinery.

[61] Alexandre Verbitski, Anurag Gupta, Debanjan Saha, Murali Brahmadesam, Kamal Gupta, Raman Mittal, Sailesh Krishnamurthy, Sandor Maurice, Tengiz Kharatishvili, and Xiaofeng Bao. Amazon Aurora: Design Considerations for High Throughput Cloud-Native Relational Databases. In *Proceedings of the 2017 ACM International Conference on Management of Data*, SIGMOD ’17, pages 1041–1052, New York, NY, USA, May 2017. Association for Computing Machinery.

[62] Giuseppe Vietri, Liana V. Rodriguez, Wendy A. Martinez, Steven Lyons, Jason Liu, Raju Rangaswami, Ming Zhao, and Giri Narasimhan. Driving cache replacement with ML-based LeCaR. In *Proceedings of the 10th USENIX Conference on Hot Topics in Storage and File Systems*, HotStorage’18, page 3. USENIX Association.

[63] Gavin Wood. Ethereum: A secure decentralised generalised transaction ledger. pages 1–32.

[64] Carole-Jean Wu, Aamer Jaleel, Will Hasenplaugh, Margaret Martonosi, Simon C. Steely, and Joel Emer. SHiP: Signature-based hit predictor for high performance caching. In *Proceedings of the 44th Annual IEEE/ACM International Symposium on Microarchitecture*, pages 430–441. ACM.

[65] Carole-Jean Wu, Aamer Jaleel, Margaret Martonosi, Simon C. Steely, and Joel Emer. PACMan: Prefetch-aware cache management for high performance caching. In *Proceedings of the 44th Annual IEEE/ACM International Symposium on Microarchitecture*, pages 442–453. ACM.

[66] Anatoly Yakovenko. Solana: A new architecture for a high performance blockchain. 2025.

[67] Xinjun Yang, Yingqiang Zhang, Hao Chen, Chuan Sun, Feifei Li, and Wenchao Zhou. PolarDB-SCC: A Cloud-Native Database Ensuring Low Latency for Strongly Consistent Reads. *Proceedings of the VLDB Endowment*, 16(12):3754–3767, August 2023.

[68] Yiyuan Yang, Rongshang Li, Qiquan Shi, Xijun Li, Gang Hu, Xing Li, and Mingxuan Yuan. SGDP: A Stream-Graph Neural Network Based Data Prefetcher.

[69] Maofan Yin, Dahlia Malkhi, Michael K. Reiter, Guy Golan Gueta, and Ittai Abraham. HotStuff: BFT Consensus with Linearity and Responsiveness. In *Proceedings of the 2019 ACM Symposium on Principles of Distributed Computing*, PODC ’19, pages 347–356. Association for Computing Machinery.

[70] Jingyu Zhou, Meng Xu, Alexander Shraer, Bala Namavayam, Alex Miller, Evan Tschannen, Steve Atherton, Andrew J. Beamon, Rusty Sears, John Leach, Dave Rosenthal, Xin Dong, Will Wilson, Ben Collins, David Scherer, Alec Grieser, Young Liu, Alvin Moore, Bhaskar Muppana, Xiaoge Su, and Vishesh Yadav. FoundationDB: A Distributed Unbundled Transactional Key Value Store. In *Proceedings of the 2021 International Conference on Management of Data*, SIGMOD ’21, pages 2653–2666. Association for Computing Machinery.

A Reth Architecture

Ethereum uses two clients: a consensus client that follows a beacon chain to determine the blockchain that is valid, and an execution client that executes the blocks from the consensus client. They work together to keep a node in sync, validate incoming blocks, and to propose new blocks. This section describes the architecture of Reth, a Rust-based high performance execution client, in particular, we focus on the block validation and execution architecture relevant to understanding our hint-based optimization. Figure 16 presents a schematic summary of the architecture that we are interested in.

A.1 System components

The execution client consists of four primary components that communicate through message-passing channels:

1. **Engine handler.** This is the central coordinator that receives block validation requests from the consensus layer and orchestrates the validation pipeline. It runs in a dedicated thread and processes requests sequentially to ensure consistency without complex synchronization. It contains two sub-components:

- *In-memory chain.* It maintains an in-memory tree of recently validated blocks indexed by block hashes. Blocks remain here until they are finalized, allowing the engine for quick-access to the current chain. It also buffers blocks with unknown parents.
- *Validator.* It validates blocks against consensus rules (format, limits, conditions) before and after the execution.

2. **Executor.** Executes transactions through the EVM and computes the post-execution state. The executor runs on a small thread pool (3 threads), and also performs operations such as transaction execution, and signature recovery from the transaction signers. It maintains a block-level cache for state access and supports speculative pre-warming by executing transactions in parallel to populate the cache before sequential execution.

3. **Block builder.** Constructs new blocks when the node is selected as proposer. The builder selects transactions from the mempool, invokes the executor to verify validity and compute gas, assembles the final block.

4. **Storage layer.** Handles durable storage of finalized blocks. Runs on a dedicated thread and receives block batches from the engine handler.

State access and caching. The executor maintains a large in-memory cache (default 9 GB) partitioned by data type:

- *Storage cache* (~ 8 GB, 89%): maps address-slot pairs to storage values. This is justified since it is the most dominant state access in smart contract execution.
- *Account cache* (~ 500 MB, 5.5%). maps addresses to account metadata (balance, nonce, code hash). While these are frequently accessed, the data per account is small.
- *Bytecode cache* (~ 500 MB, 5.5%). maps code hashes to contract bytecode. The values in these cache are immutable, but individual contracts can be large, e.g., 24 KB.

The cache uses time-based eviction with a 2-hour time-to-live and 1-hour idle timeout. Entries are weighted by their actual memory footprint rather than count, ensuring the memory budget is respected regardless of entry size.

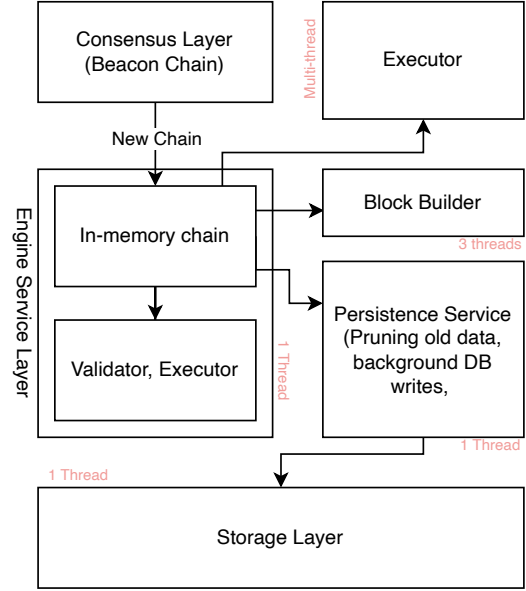


Figure 16: Reth architecture for block production and validation

Cache misses fall through to MDBX. Historical data (old blocks, transactions, receipts) is stored in separate immutable files to reduce database size and improve locality for recent state.

A.2 Storage

In this section, we focus on the storage layers relevant to the state access for block execution. Reth’s storage layer uses three categories of tables to serve both current and historical state queries.

Plain State Tables. These store the current state of the chain. These tables are updated as new blocks are executed and represent the most recent state.

Plain Account State Tables. These map each address to its current account (balance, nonce, code hash).

Plain Storage State. These map each (address, slot) pair to its current storage value.

Change Set Tables. These record what changed in each block, storing the value before the change. Together, change sets enable *time travel*, i.e., to recover the state at any historical block, one can start from the current plain state and walk backwards through change sets.

Account Change Sets. These are keyed by block number and stores the previous account state for every account modified in that block.

Storage Change Sets. is keyed by (block number, address) and stores the previous storage value for every slot modified in that block.

History Index Tables. These provide efficient lookups to find which blocks modified a given key, avoiding a linear scan through change sets. The bitmaps use roaring bitmap compression and are sharded into chunks of 2,000 entries for bounded per-entry size.

Accounts History. These map each address to a compressed bitmap of block numbers where that address was modified.

Storage History. maps each (address, slot) pair to a compressed bitmap of block numbers where that slot was modified.

A.3 MDBX database

All tables described above are stored in MDBX [9], an embedded key-value database derived from LMDB. MDBX organizes data in B^+ -trees and uses memory-mapped I/O to expose database pages directly in the process address space. Rather than issuing explicit read system calls, Reth accesses database pages by dereferencing pointers into the mapped region; the operating system’s virtual memory subsystem transparently faults in pages from disk on demand.

Implications for performance. This design has two consequences that are central to our optimization. First, the cost of a database read depends on whether the accessed page resides in the OS page cache. A warm read (page already cached) completes with a page-table walk and a memory load, while a cold read triggers a page fault that blocks the calling thread until the page is read from storage. Because MDBX does not maintain its own buffer pool, the OS page replacement policy governs the eviction, which has no knowledge of the application’s access pattern. Second, each historical state lookup traverses a B^+ tree in the history index table, touching $O(\log n)$ pages, any of which may trigger a page fault. Under memory pressure or when the working set exceeds available RAM, these random traversals incur multiple storage round-trips per lookup. Our system Ira-L tackles this bottleneck by supplying source hints that eliminate redundant index traversals.

Why multi-threaded prefetching is necessary. Although Ira’s hints identify exactly which keys will be accessed, prefetching them efficiently is complicated by MDBX’s use of memory-mapped I/O. Because reads are pointer dereferences into the mapped region rather than explicit system calls, a cold page access manifests as a synchronous page fault that blocks the faulting thread until the kernel completes the I/O. There is no mechanism to issue an asynchronous read against an `mmap`’d region from user space. While `madvise(MADV_WILLNEED)` [10] can hint to the kernel that pages will be needed soon, it is purely advisory: the kernel may defer or ignore the request, and critically, it provides no completion notification, so the application cannot determine

when pages are actually resident. A single-threaded prefetcher would therefore serialize all page faults, issuing at most one storage read at a time and failing to exploit the parallelism available in modern NVMe devices (which support tens of thousands of concurrent I/O operations). To overcome this, Ira-L dispatches prefetch requests across a pool of threads: each thread touches a different B^+ -tree path, absorbs its own page fault independently, and the OS services the resulting I/O requests concurrently through the NVMe submission queue. This helps reduce the impact of our inability to prefetch data.

A.4 Reth Baseline Architecture

We build a benchmark tool that replays historical blocks to measure execution performance. It simulates production behavior for block validators.

Components.

- *Block Processor.* Iterates through blocks sequentially, coordinating the per-block cache and executor for each block. Records execution time and memory usage.
- *Per-Block Cache.* A temporary cache created fresh for each block. During execution, it accumulates all state accessed by transactions (accounts, storage slots, bytecode). The executor reads and writes state through this cache. After the block completes, its contents are merged into the cross-block cache.
- *Executor.* Runs transactions sequentially through the EVM. Reads state from the per-block cache and writes resulting state changes back to it.
- *Cross-Block Cache.* A persistent LRU cache that survives across blocks. Contains:
 - Accounts (100K entries)
 - Storage slots (1M entries)
 - Bytecode (10K entries)

When the per-block cache encounters a miss, it queries the cross-block cache. After each block, touched state is merged back, so block $N+1$ benefits from state accessed during block N .

- *Storage.* The underlying database (reth’s MDBX) opened in read-only mode. The cross-block cache queries storage on cache misses to fetch historical state.

Data Flow.

1. The block processor initializes a fresh per-block cache and invokes the executor
2. The executor reads and writes state through the per-block cache

3. On cache miss, the per-block cache queries the cross-block cache
4. On cache miss, the cross-block cache queries storage
5. After execution completes, the per-block cache contents are merged into the cross-block cache
6. The process repeats for the next block

B Ira-L Architecture

In this section, we provide details of Ira-L implementation in Rust.

B.1 Reth Primary

reth-primary is the hint generator that simulates a block proposer. It replays blocks, collects all state keys accessed during execution, and writes hints that enable other backups to prefetch state for faster replay. Figure 17 presents an illustration of our architecture. **Components**.

1. *Block Processor*: Iterates through blocks sequentially, coordinating execution, hint construction, and output writing.
2. *Key Collector*: An EVM inspector that records accessed keys by intercepting opcodes:
 - SLOAD/SSTORE: storage slot accesses
 - BALANCE/SELFBALANCE: account accesses
 - CALL/STATICCALL/DELEGATECALL: bytecode accesses
 - EXTCODECOPY/EXTCODESIZE: bytecode/account accesses
3. *Executor*: Runs transactions through the EVM with the inspector from the Key Collector attached. The inspector intercepts EVM opcodes to capture all state accesses without modifying execution behavior.
4. *Source Tracker*: For each storage key, queries the storage history index to determine the optimal read source:
 - Plain State: We write the value 0 to indicate the current value in main state table.
 - Not Yet Written: We write the value 1 to indicate that the slot was never written and its value is zero.
 - Changeset: We write the value 2 to indicate that this value must be read from historical change sets.

This source annotation allows validators to route prefetch requests optimally. Without source hints, in order to read a storage value at a historical block, the validator must perform the full two-step lookup for every key:

- (a) History index seek. Seek in Storage History for the (address, slot) pair. This involves a B-tree traversal on a 60-byte composite key, followed by roaring bitmap decompression and a rank/select operation.
- (b) Value fetch. Based on the history index result, read from either Plain Storage State, Storage Change Sets, or return zero.

Step 1 is expensive since it is a random B-tree seek into a large index table, and it must be done for every key. We observed that the answer is often "read from Plain State" or "the value is zero." Using Plain State, the validator skips the history index entirely and reads directly from Plain Storage State. This eliminates one B-tree seek per key. Using Not Yet Written, the validator skips all disk I/O. The value is known to be zero without touching the database. Using Changeset, we get no savings, and the validator must perform the full historical lookup.

As we observe in our analysis, the majority of storage accesses in a typical block hit keys that have not been modified recently, i.e., their current value in Plain State is correct for the historical block being queried. For these keys, the history index lookup is pure overhead: it exists only to confirm that Plain State is the right source. The source hint eliminates that confirmation step. In the best case (Plain State), the hint converts a two-seek operation into a one-seek operation. In the zero case (Not Yet Written), it eliminates disk access entirely. Only keys in the Changeset category still pay full cost.

5. *Hint Constructor*: Assembles the final Block Hints structure containing storage keys (with sources), account addresses, and bytecode addresses.
6. *Hint Writer*: Persists hints to a redb database [21] with zstd [26] compression.

Data Flow.

1. Block processor fetches block from storage.
2. Executor runs transactions with Key Collector inspector.
3. Key Collector captures all accessed keys via opcode interception.
4. Source tracker queries storage history to annotate each key with its optimal read source.
5. Hint constructor assembles the complete hint set.
6. Hint writer persists hints; state hash writer records execution fingerprint.

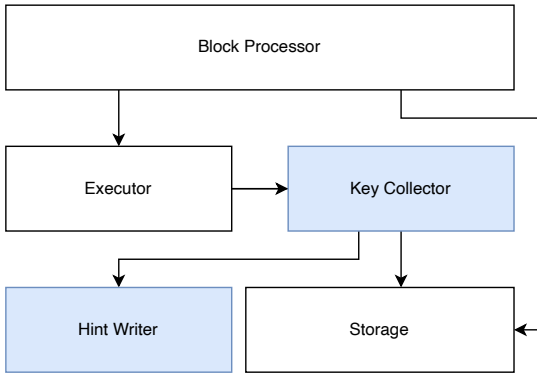


Figure 17: Architecture of our implementation of Ira-L primary. The components marked in blue are the proposed changes to the primary.

B.2 Reth Backup

reth-backup is the hint consumer that simulates a validator receiving hints from the proposer. It prefetches all required state before execution, so that block processing incurs zero disk I/O. Figure 18 presents an illustration of our architecture.

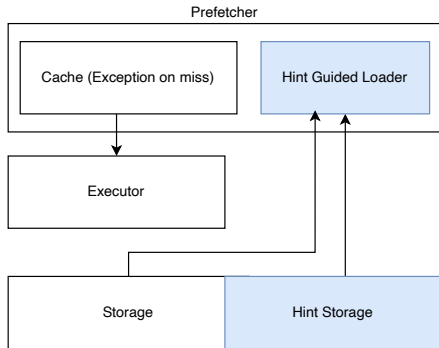


Figure 18: Architecture of our implementation of Ira-L backup. The components marked in blue are proposed changes to the backup.

Components.

1. *Prefetcher*: Runs on a dedicated thread and loads state ahead of execution in two phases:
 - *Phase 1 (startup)*: Prefetches 3,000 blocks in parallel using rayon (configurable number of threads), filling an 8 GB in-memory buffer. This covers the initial cold start.
 - *Phase 2 (steady-state)*: Prefetches in sorted batches of 32 blocks. For each batch, it collects

all keys from all blocks, sorts them by address, and reads them using forward cursor walks. This converts random I/O into sequential I/O across the B-tree. Prefetched blocks are sent to the executor via a bounded channel.

Hint-Guided Loader: The core of the prefetcher. For each batch of hints, it routes reads by source annotation:

- Plain State: Read directly from the plain state table using a sorted cursor. This is the fast path (90% of keys).
- Not Yet Written: Insert zero immediately. No disk access.
- Changeset: Skipped during prefetch. These rare keys fall back to on-demand reads.

The loader also reads account metadata and bytecode, sorting keys before reading to maintain sequential access patterns.

2. *Executor*: Consumes pre-populated blocks from the prefetcher. Each block arrives with a cache containing all required state. Execution runs through the EVM with no disk access. The cache is backed by a DB that causes an exception if it does not contain a key: if execution attempts to read a key not in the cache, it crashes, verifying that the hints provide complete coverage. Each cache is discarded after execution to prevent memory accumulation simulating a conservative approach.
3. *Storage*: The reth database is accessed only by the prefetcher thread, never during execution. Only three tables are used: Plain Account State, Plain Storage State, and Bytecodes.

Threading Model. The prefetcher and executor run on separate threads, connected by a bounded channel (capacity 100 blocks). This pipelining ensures the executor never waits for I/O: while it executes block N , the prefetcher is loading state for block $N + 1$ and beyond. The 8 GB buffer absorbs variance in prefetch and execution times.

Key Design Decisions.

1. Sorted batch reads. By collecting keys from 32 blocks, sorting, and reading in order, the prefetcher converts random B-tree seeks into forward cursor walks. This is significantly faster on both SSDs and HDDs.
2. No cross-block cache. Unlike reth-baseline, the backup discards each block's cache after execution. Hints make the cross-block cache unnecessary since every block's state is prefetched independently.
3. DB that throws exceptions as a safety net. Using a crashing fallback database instead of a real one guarantees that execution timing measurements are not contaminated by unexpected disk I/O.

C Additional Details

Table 5 provides detailed bucketed statistics for the intra-block access frequency distribution shown in Figure 5. Table 6 provides the detailed breakdown for the contract concentration shown in Figure 6. Table 7 provides the detailed breakdown for the key lifespan distribution shown in Figure 7. Table 8 provides per-block statistics shown in Figure 8. Section C.1 provides the source annotation distribution referenced in Section 4.1. Section C.2 provides the tabulated backup speedup and tail behavior data. Section C.3 provides a detailed analysis of hint cost scaling and variance.

Table 5: Intra-block access distribution: how many times each key is accessed within its block.

Accesses per Key	Block-Key Pairs	Share
1	69,264,600	34.5%
2	63,445,255	31.6%
3–5	49,614,494	24.7%
6–10	12,665,780	6.3%
> 10	5,848,961	2.9%

Table 6: Cumulative storage access share by contract rank.

Top-N Contracts	Cumulative Share
Top 1 (USDT)	16.5%
Top 2 (+USDC)	31.4%
Top 3 (+Compound)	42.2%
Top 10	63.6%
Top 20	67.4%

Table 7: Key lifespan distribution: number of blocks in which each key appears.

Blocks Appeared	Keys	Share
1 block	25,382,837	72.4%
2–5 blocks	7,497,511	21.4%
6–20 blocks	1,413,794	4.0%
21–50 blocks	385,501	1.1%
> 50 blocks	356,088	1.0%

C.1 Source Annotation Distribution

Each storage key in the hint carries a one-byte source annotation indicating where the backup should read its value (Section 4.1). Table 9 reports the aggregate distribution across all 200,828,943 storage key accesses in the dataset.

PlainState keys (46.6%) require a single B-tree seek; Zero keys (10.5%) require no I/O at all; only Changeset keys

Table 8: Per-block storage statistics.

Metric	Median	P95	Max
Total operations	8,629	24,644	109,627
Storage operations	6,587	19,058	77,876
Unique storage keys	1,806	3,920	10,258

(43.0%) require the full two-step history lookup. In total, 57.0% of storage keys bypass the history index entirely.

The per-block distribution is stable: PlainState has a median share of 47.5% (IQR 43.5–50.9%), Zero has a median of 5.6% (IQR 4.0–9.2%), and Changeset has a median of 44.7% (IQR 39.7–48.6%).

Table 9: Source annotation distribution across storage keys.

Source	Keys	Share	Per-Block Median
PlainState	93,546,384	46.6%	47.5%
Zero	21,016,404	10.5%	5.6%
Changeset	86,266,155	43.0%	44.7%
No history (PlainState + Zero)	–	57.0%	55.3%

C.2 Backup Speedup Details

Table 10 provides the per-block speedup percentiles summarizing Figure 13. Table 11 provides the tail behavior breakdown referenced in Section 5.3.2.

Table 10: Per-block speedup distribution (backup vs. baseline).

Configuration	Median	P90	P99	Max
Sequential	24.9×	45.0×	103.0×	895.9×
Parallel-16	24.4×	44.2×	100.3×	750.7×
Parallel-64	24.8×	44.8×	102.8×	856.6×

C.3 Hint Cost Variance Analysis

The per-block hint fraction (Figure 9) varies across blocks despite a stable per-key cost. Table 12 shows how the hint fraction changes with block working set size. The median hint fraction decreases monotonically from 24.8% for small blocks (<500 keys) to 9.7% for large blocks (>5K keys), even though absolute hint time increases. This occurs because execution time grows faster than hint time for larger blocks: large blocks perform more I/O, and the I/O-dominated execution time scales super-linearly with working set size while hint construction scales linearly (Figure 10).

Variance decomposition. To identify the dominant source of per-block hint fraction variance, we fix each component

Table 11: Fraction of blocks where backup is slower than baseline.

Configuration	Slower Blocks	Fraction
Sequential	3,047	3.02%
Parallel-16	252	0.25%
Parallel-64	91	0.09%

Table 12: Hint cost breakdown by block working set size.

Unique Keys	Blocks	Hint Frac. (median)	Exec Time (median)	Hint Time (median)
<500	3,195	24.8%	53 ms	13.0 ms
500–1K	4,787	15.0%	123 ms	16.8 ms
1K–2K	28,409	12.7%	206 ms	24.8 ms
2K–3K	15,846	10.8%	327 ms	34.7 ms
3K–5K	6,753	9.8%	440 ms	42.5 ms
>5K	194	9.7%	536 ms	52.0 ms

at its median and measure the resulting variance reduction. Fixing execution time at its median reduces hint fraction variance by 65%, confirming that I/O-driven execution time variability, not hint cost variability, is the primary source of per-block fluctuations. Fixing serialization time at its median reduces variance by 28%, consistent with the observation that serialization exhibits occasional latency spikes from disk contention while maintaining a tight steady-state distribution (IQR 11.9–13.1 ms).

Serialization cost. Serialization time is dominated by the fixed overhead of committing the database write transaction (opening, flushing, and closing the redb write batch), not by the volume of data written. This explains the near-zero correlation with block size ($r = 0.03$). The tight IQR (11.9–13.1 ms) indicates stable steady-state performance, with rare spikes attributable to background disk I/O contention from the concurrent MDBX database.

D Generalized Ira Architecture

In this appendix, we present the generalized Ira protocol that can be adapted to any primary-backup system with a key-value store interface, and provide sketches for integrating Ira into production systems.

D.1 Abstract Protocol

System Model. Consider a primary-backup replication system where:

- State is stored as a key-value map $S : \mathcal{K} \rightarrow \mathcal{V}$
- Transactions are batches of operations $T = \langle op_1, \dots, op_n \rangle$ where each op_i is either $READ(k)$ or $WRITE(k, v)$

Algorithm 3 Generalized Ira Hint Generation (Primary)

Require: Transaction batch $T = \langle op_1, \dots, op_n \rangle$, State S
Ensure: Hint H , Execution result R

```

1:  $A \leftarrow \emptyset$  // Access set
2: for  $i \leftarrow 1$  to  $n$  do
3:   if  $op_i = \text{READ}(k)$  then
4:      $A \leftarrow A \cup \{k\}$ 
5:     Execute read from  $S$ 
6:   else if  $op_i = \text{WRITE}(k, v)$  then
7:      $A \leftarrow A \cup \{k\}$ 
8:     Execute write to  $S$ 

9:  $M \leftarrow \text{COMPUTEMETADATA}(A, S)$  // Optional: sources,
   ordering
10:  $H \leftarrow (A, M)$ 
11: return  $(H, R)$ 

```

- The primary executes transactions and propagates them to backups via a replicated log
- Backups replay transactions from the log to maintain consistent state

Hint Generation (Primary). During execution of transaction batch T , the primary maintains an access set $A = \emptyset$. For each operation:

- $READ(k)$: Add k to A
- $WRITE(k, v)$: Add k to A (writes typically require reading the old value for logging or conflict detection)

After execution, the primary constructs hint $H = (A, M)$ where M is optional metadata (source annotations, access ordering, etc.). The primary transmits H alongside or ahead of T to backups.

Hint-Based Prefetch (Backup). Upon receiving hint $H = (A, M)$, the backup:

1. Sorts A by key order to enable sequential I/O through the storage engine’s B-tree or LSM index
2. For each $k \in A$, fetches $S[k]$ into an in-memory cache
3. If M contains source annotations, routes reads to the appropriate storage tier (e.g., main table vs. historical snapshots)

Replay (Backup). The backup executes transaction T with all keys pre-cached. All $READ(k)$ operations return immediately from cache; $WRITE(k, v)$ operations update the cache and mark entries dirty for eventual persistence.

Algorithms 3 and 4 present the generalized hint generation and replay algorithms.

Algorithm 4 Generalized Ira Replay (Backup)

Require: Transaction batch T , Hint $H = (A, M)$, State S
Ensure: Updated state S'

```
// Phase 1: Prefetch via sorted sequential scan
1:  $A' \leftarrow \text{SORTBYKEY}(A)$ 
2:  $cache \leftarrow \emptyset$ 
3: for  $k \in A'$  do
4:    $cache[k] \leftarrow S[k]$  // Sequential I/O

// Phase 2: Execute with all state in cache
5: for  $op \in T$  do
6:   if  $op = \text{READ}(k)$  then
7:     return  $cache[k]$  // Cache hit
8:   else if  $op = \text{WRITE}(k, v)$  then
9:      $cache[k] \leftarrow v$ 
10:    Mark  $k$  as dirty

// Phase 3: Persist dirty entries
11: for  $k \in cache.\text{DIRTY}()$  do
12:    $S[k] \leftarrow cache[k]$ 
```

D.2 Hint Transmission Strategies

The protocol admits several transmission strategies with different tradeoffs:

Inline Transmission. Transmit hint H as part of the log entry containing transaction batch T . This is the simplest approach: hints and transactions are atomically committed and delivered together. The cost is increased log entry size, which may affect replication latency for bandwidth-constrained networks.

Sideband Transmission. Transmit hint H through a separate channel ahead of transaction T . This allows backups to begin prefetching before the transaction arrives, hiding prefetch latency behind network transmission time. The cost is coordination complexity: backups must match hints to their corresponding transactions, and hints may arrive out of order or be lost independently.

On-Demand Transmission. Backups request hints from the primary only when they detect high cache miss rates. This reduces bandwidth when the workload exhibits high locality (most keys are already cached), but increases latency when hints are needed. Suitable for systems with variable workload patterns.

D.3 System-Specific Integration Sketches

Apache Kafka (Kafka Streams). Kafka Streams applications maintain local state stores (typically backed by RocksDB) that are updated during record processing. When a consumer falls behind, it must replay records while performing state store lookups that may miss the RocksDB block cache.

Integration. The producing application, which knows what

state store keys each record will access, attaches the access set as a record header. Consumers extract the header and prefetch state store entries before processing each batch. For changelog-backed state stores, hints can be derived from the changelog records themselves, with each changelog entry implying a future read of that key.

Raft-Based Systems (etcd, TiKV, CockroachDB). In Raft, the leader executes commands and replicates log entries to followers. Followers apply log entries to their local state machine, typically backed by RocksDB or a similar embedded database.

Integration. The leader's state machine execution already observes key accesses. Extend the Raft log entry format to include an optional access set field. Followers extract the access set and prefetch from their local RocksDB instance before applying the entry. This is particularly valuable during leader failover: the new leader must replay any uncommitted entries, and hint-based prefetching accelerates this recovery path.

PostgreSQL Streaming Replication. PostgreSQL standbys apply Write-Ahead Log (WAL) records streamed from the primary. Each WAL record describes changes to specific heap pages and index pages. Replay performance depends on whether the required pages are in the standby's buffer pool.

Integration. The primary's buffer manager observes which pages are accessed during transaction execution. Extend the WAL protocol to include page-level access lists, either per-record or aggregated per checkpoint interval. Standbys use these lists to prefetch pages from disk into their buffer pool before applying WAL records. This is especially valuable for standbys with smaller buffer pools than the primary or after standby restart when the buffer pool is cold.

MySQL Group Replication / Galera Cluster. MySQL replication uses binary log (binlog) events that describe row-level changes. Replicas apply these events by locating affected rows through index lookups, which may incur cache misses in the InnoDB buffer pool.

Integration. During binlog event creation, the primary observes which index pages are traversed for each row operation. Extend the replication protocol to include these page identifiers as hints. Replicas prefetch the indicated pages into their buffer pool before applying the binlog event. For certification-based replication (Galera), hints can be attached to the writeset certification request.

Distributed Key-Value Stores (FoundationDB, TiKV). These systems use consensus-based replication where storage servers replay the leader's mutation log. The leader (or transaction coordinator) knows exactly which keys each transaction reads and writes.

Integration. FoundationDB's storage servers receive mutation batches from the transaction log. Extend the mutation batch format to include the read set (keys read during transaction execution) in addition to the write set. Storage servers prefetch read-set keys from their local SQLite or RocksDB instance

before applying mutations. TiKV can similarly extend its Raft log entries with read-set hints, enabling followers to prefetch before applying proposals.

D.4 Hint Sizing and Bandwidth Considerations

Key Representation. For systems with structured keys (e.g., $(table, row, column)$ tuples or composite keys with common prefixes), hints can be compressed:

- **Prefix compression:** Many keys share common prefixes (same table, adjacent rows). Store the common prefix once and encode suffixes differentially.
- **Bloom filters:** For approximate prefetching, encode the access set as a Bloom filter. False positives cause unnecessary prefetches (wasted I/O) but false negatives are impossible and all the accessed keys will be prefetched.
- **Range encoding:** For range scans, encode $(start, end)$ rather than enumerating individual keys.

Bandwidth-Latency Tradeoff. Let B_H be the hint bandwidth cost (bytes per transaction) and ΔL be the replay latency reduction from hint-based prefetching. The system benefits from hints when:

$$\frac{B_H}{\text{bandwidth}} < \Delta L \cdot |\text{backups}|$$

For high-fanout replication (many backups), even moderately expensive hints become worthwhile because the primary generates hints once but multiple backups benefit. Ira-L (Section 4) achieves median hint sizes of 46.5 KB per block which is comparable to a few TCP packets, while providing 24.9 \times median speedup.

Adaptive Hint Granularity. Systems can dynamically adjust hint detail based on observed conditions:

- **High cache hit rate:** Reduce hint detail or disable hints entirely. The workload has sufficient locality that standard caching policies perform well.
- **High cache miss rate:** Increase hint detail (add source annotations, access ordering). The workload is random or the working set exceeds cache capacity.
- **Network congestion:** Switch to lossy representations (Bloom filters, sampled access sets) that trade prefetch accuracy for reduced bandwidth.